Poly(1,6-heptadiyne), a Free-Standing Polymer Film Dopable to High Electrical Conductivity[1]

Harry W. Gibson,*† F. C. Bailey,† Arthur J. Epstein,† Heiko Rommelmann,† Samuel Kaplan,† John Harbour,‡ Xiao-Quing Yang,§,‖ David B. Tanner,§,‖ and John M. Pochan†,⊥

Contribution from the Webster Research Center, Xerox Corporation, Webster, New York 14580, the Xerox Research Centre of Canada, Mississauga, Ontario L5L 1J9, Canada, and the Department of Physics, The Ohio State University, Columbus, Ohio 43210.
Received September 7, 1982

Abstract: Polymerization of 1,6-heptadiyne on the surfaces of concentrated solutions of homogeneous Ziegler-Natta catalysts leads to insoluble, free-standing films with metallic luster. "Doping" of these films by treatment with acceptors results in conductivities up to 1 S/cm. The polymer has been characterized in terms of its molecular structure, its solid-state structure and physical properties, the nature of the doping process, and its thermal and oxidative stability. Poly(1,6-heptadiyne) provides a number of contrasts to polyacetylene in its molecular and solid-state structure which yield some information about the requirements for conductive polymers.

Electrically conductive polymers have been the subject of sporadic interest for at least the last 25 years.[2,3] The discovery of a method of preparation of free-standing films of polyacetylene[4] sparked a rebirth of interest in this conjugated polyene that had been previously studied in powder form.[5] The films were more amenable to study of physical properties and for many potential applications. A number of dopants were subsequently found to be effective for raising the conductivity into the metallic regime.[6]

At the inception of the present study, no other substituted polyenes had been formed as films in situ during polymerization. Our initial goal was to determine whether other conjugated polyenes could first be polymerized in situ to free-standing films and then doped to high electrical conductivity. If this goal could be reached, optimization of properties such as flexibility, ductility, thermal transitions, oxidative stability, etc. might be achieved by modification of substituents on the polyene chain. It was known,[7] however, and subsequently confirmed by using the Shirakawa catalyst[8] that substituted acetylenes, e.g., methyl and ethyl derivatives, polymerize sluggishly in comparison to acetylene itself. Because cyclopolymerization was of such utility in the synthesis of substituted olefin derived polymers,[9] it was our belief that cyclopolymerization of diacetylenes might prove useful in the preparation of substituted polyacetylenes.

The polymerization of 1,6-heptadiyne (**1**) using an insoluble

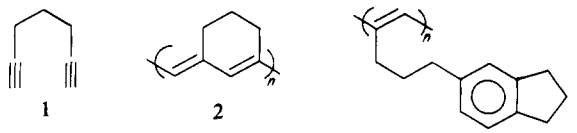

1 **2** **3**

Ziegler-Natta catalyst [$TlCl_4/Al(i\text{-}C_4H_9)_3$] was reported by Stille and Frey.[10,11] The resultant polymer was soluble. Its structure was proposed to be **2**, the six-membered ring-containing polyene. This structure was later rejected by other workers in favor of **3**, resulting from cyclotrimerization prior to polymerization.[12] For our purposes either **2** or **3** was suitable, and we undertook a study aimed at preparation of this polymer in situ as free-standing film and characterization of its properties. This paper summarizes the results of these efforts.

Discussion

(A) Synthesis. Our initial attempts to synthesize films of poly(1,6-heptadiyne) ("poly-1,6") utilized the "Shirakawa catalyst,"[4] a homogeneous catalyst derived from $Ti(OC_4H_9\text{-}n)_4$ and $Al(C_2H_5)_3$. These experiments were successful in producing films.

Table I. Effect of Catalyst Composition $Ti(OR)_4$ Plus $Al(C_2H_5)_3$[a]

R	result	yield, %
$n\text{-}C_4H_9$	golden-green lustrous somewhat flexible film	69
$i\text{-}C_3H_7$[b]	golden-green lustrous film (small amount) plus dull black thick film in bottom of reactor	~5 + ~85
$n\text{-}C_9H_{19}$	golden-green lustrous somewhat flexible film	60

[a] 4.0/1.0 $Al(C_2H_5)_3/Ti(OR)_4$; $[Ti(OR)_4] = 0.18$ M in toluene; reactor 20 °C; monomer 50 °C; catalyst prepared and aged 1 h at 25 °C; degassed 6× to $P \simeq 4 \times 10^{-4}$ torr at −78 °C; wash solvent = toluene. [b] Catalyst had low viscosity.

Table II. Effect of Catalyst Composition $Ti(OC_4H_9\text{-}n)_4$ Plus AlR_3[a]

R	solvent	[Ti], M	reactor temp, °C	result
C_2H_5	toluene	0.43	20	golden-green "metallic" film
C_2H_5	hexane	0.32	20	very little film (thin)
CH_3	hexane	0.47	5	no film
$i\text{-}C_4H_9$	toluene	0.25	19	no film

[a] Al/Ti = 4.0. Monomer 48 ± 3 °C; catalyst prepared and aged 1 h at 25 °C; degassed 6× to $P = 6 \times 10^{-4}$ torr at −78 °C; wash solvent = toluene.

† Webster Research Center.
‡ Xerox Research Centre of Canada.
§ Department of Physics.
‖ Present address: Department of Physics, University of Florida, Gainesville, FL.
⊥ Present address: Research Laboratories, Eastman Kodak Company, Rochester, NY 14650.

(1) A portion of this work has been communicated: H. W. Gibson, F. C. Bailey, A. J. Epstein, H. Rommelmann, and J. M. Pochan, *J. Chem. Soc., Chem. Commun.*, 426 (1980).
(2) C. B. Duke and H. W. Gibson, "Encyclopedia of Chemical Technology", Wiley, New York, 1982, Vol. 18, pp 755–794.
(3) H. W. Gibson, *Polymer*, in press.
(4) T. Ito, H. Shirakawa, and S. Ikeda, *J. Polym. Sci., Polym. Chem. Ed.*, **12**, 11 (1974).
(5) M. Hatano, S. Kambara, and S. Okamoto, *J. Polym. Sci.*, **51**, 526 (1961). D. J. Berets and D. S. Smith, *Trans. Faraday Soc.*, **64**, 823 (1968).
(6) C. K. Chiang, A. J. Heeger, and A. G. MacDiarmid, *Ber. Bunsenges. Phys. Chem.*, **83**, 407 (1979). A. G. MacDiarmid and A. J. Heeger, *Synth. Met.*, **1**, 101 (1980), and references cited therein. A. J. Epstein, H. Rommelmann, and H. W. Gibson, *Mater. Sci.* **7**, 133 (1981). See also: A. J. Epstein and E. M. Conwell, Eds., *Mol. Cryst. Liq. Cryst.*, **77** (1981) and **83** (1982) for recent work.
(7) V. Enkelmann, W. Muller, and G. Wegner, *Synth. Met.*, **1**, 185 (1980). W. H. Watson, W. C. McCordie, and L. G. Lands, *J. Polym. Sci.*, **55**, 137 (1961). P. S. Woon and M. F. Farona, *J. Polym. Sci., Polym. Chem. Ed.*, **12**, 1749 (1974).

0002-7863/83/1505-4417$01.50/0

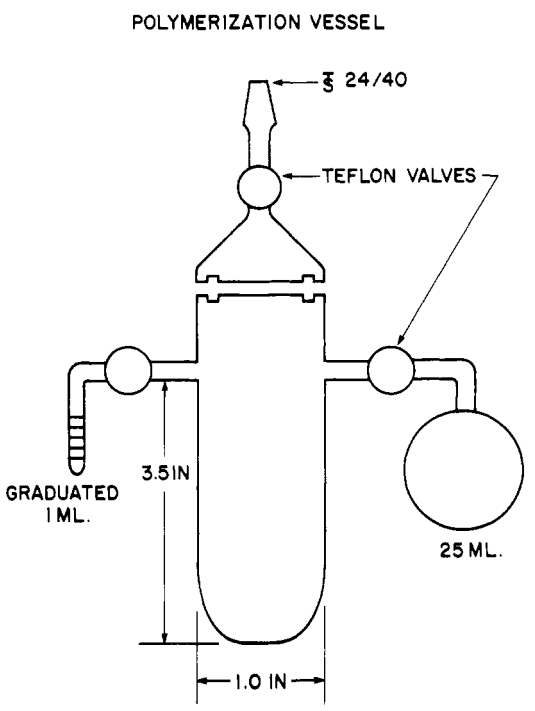

Figure 1. Reaction vessel for polymerization of 1,6-heptadiyne to insoluble free-standing film.

Table III. Effect of Catalyst Ratio Using $Ti(OC_4H_9\text{-}n)_4$ and $Al(C_2H_5)_3$[a]

Al/Ti	result	yield, %
1.0[b]	dull black, brittle film; much soluble material	57
4.0	golden-green, lustrous, somewhat flexible film	69
10.0	very thin film	6

[a] $[Ti(OC_4H_9\text{-}n)_4]$ = 0.18 M in toluene; monomer 48 ± 1 °C unless otherwise stated; reactor 20 °C; wash solvent = toluene. [b] Monomer 39 °C.

We then turned our attention to systematic study of the reaction variables.

For these experiments we utilized reactors of the type shown in Figure 1. A graduated side arm is provided for the monomer and a bulb for the wash residues, both separated from the reactor proper by Teflon valves. The catalyst solutions, prepared in an oxygen- and water-free glovebox, were degassed on a vacuum line after aging. After removal from the vacuum line, the reactor proper and the monomer were then thermostated individually. After the reactor walls were coated with a film of catalyst, monomer was admitted. After polymerization, washing was accomplished by decantation of solvent (previously distilled into the wash bulb) out of the reactor into the side bulb followed by distillation back into the reactor. The film, after vacuum drying, was removed and weighed in the glovebox.

(1) Effectiveness of Catalyst Components. (a) Variation of Titanium Alkoxide. Table I shows the results of experiments with titanium(IV) *n*-butoxide, isopropoxide, and *n*-nonylate. The *n*-alkoxides gave a golden-green lustrous film in comparable yield, but the branched alkoxide yielded primarily a black residue as a result of polymerization in the catalyst pool rather than on the reactor walls, perhaps the result of the catalyst's low viscosity. In view of the ease of purification of the *n*-butoxide, it was chosen for the other experiments.

(b) Variation of Aluminum Alkyl. Table II displays the results for various aluminum alkyl/solvent combinations when reacted with titanium tetra(*n*-butoxide). Only triethylaluminum in toluene yielded the lustrous polymer films. Hexane's vapor pressure is probably a factor in the failure of both $Al(C_2H_5)_3$/hexane and $Al(CH_3)_3$/hexane to bring about polymerization in film form.

(c) Effect of $Ti(OC_4H_9\text{-}n)_4/Al(C_2H_5)_3$ Ratio. In Table III the results of variation of the Al/Ti ratio from 1 to 10 are recorded. High ratios (~10) give poor film yields, while ratios between 1 and 4 afford 60–70% yields.

(2) Effect of Reaction Temperature. Variation in the reaction temperature (Table IV) has a profound effect upon polymer film

Table IV. Effect of Reaction Temperature[a]

reactor temp, °C	monomer temp, °C	result	yield, %
−78	88 or 50	no film formation	
−37	34	golden-green, lustrous thin flexible film; low yield; much soluble material	~10
0	40	golden-green, lustrous thick film; moderate flexibility; very little soluble material	100
20	49	golden-green, lustrous somewhat flexible film; some soluble material	69
48	76	golden-green, lustrous somewhat flexible film; some soluble material	75

[a] 4.0/1.0 $Al(C_2H_5)_3/Ti(OC_4H_9\text{-}n)_4$; [Ti] = 0.18 M in toluene; wash solvent = toluene.

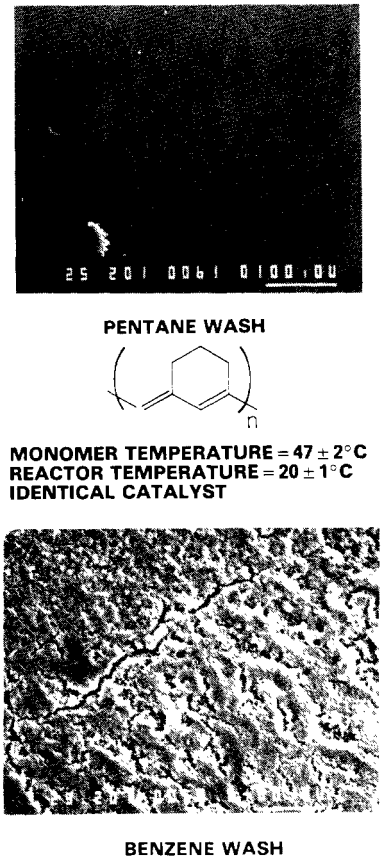

Figure 2. Scanning electron micrographs of poly(1,6-heptadiyne) films washed with pentane (top) and benzene (bottom). Solid bars in lower right corners are 1 μm.

(8) J. C. W. Chien, G. E. Wnek, F. E. Karasz, and J. A. Hirsch, *Macromolecules*, **14**, 479 (1981).
(9) G. B. Butler, G. C. Corfield, and C. Aso, *Prog. Polym. Sci.*, **4**, 71 (1975). G. B. Butler and R. J. Angelo, *J. Am. Chem. Soc.*, **79**, 3128 (1957). G. B. Butler, A. Crawshaw, and W. L. Miller, *J. Am. Chem. Soc.*, **80**, 3615 (1958).
(10) J. K. Stille and D. A. Frey, *J. Am. Chem. Soc.*, **83**, 1697 (1961).
(11) We thank Prof. H. Hall, University of Arizona, for pointing out ref 10 to us.
(12) A. J. Hubert and J. Dale, *J. Chem. Soc.*, 3160 (1965).
(13) E. C. Colthrup and L. S. Meriwether, *J. Org. Chem.*, **26**, 5169 (1961).

Table V. Elemental Analytical Data for Poly(1,6-heptadiyne)[a]

% C	% H	% ash	C/H, 7.00/x
87.41[b]	8.71	3.00	8.28
89.71[c]	8.92	2.81	8.29
86.46[d]	8.42	1.88	8.12
87.72[e]	8.44	3.53	8.02
85.06[f]	8.57	2.86	8.40

[a] Calculated for $(C_7H_8)_n$: C = 91.25%; H = 8.75%. Pentane- or toluene-washed unless otherwise noted. [b] Average of 15 samples. SD: C, ±1.04; H, ±0.23; ash, ±0.67; C/H, x ±0.24. [c] Highest percent C sample. [d] Lowest percent ash sample; washed with toluene by soaking 11 days with occasional decantation and redistillation. [e] Best C/H ratio sample. [f] Tetrahydrofuran/methanol (6/1) wash.

Table VI. Elemental Analyses of a Sample of Poly(1,6-heptadiyne) Undoped and Doped prior to Refinement of Handling Techniques by Analytical Laboratories

sample	% C	% H	% O	% As	% F	% I	total
undoped[a]	68.29	7.39	24.15				99.83
undoped[a,b]	68.09	7.28					
AsF_5 doped[a,c]	61.14	6.30		13.46	17.14		98.04
undoped[d,e]	82.26	8.74	9.14				100.14
I_2 doped[d,f]	67.80	6.84				23.05	97.69

[a] Laboratory A. [b] Same sample as in footnote *a* analyzed 2 weeks later. [c] Empirical formula: $C_{7.00}H_{8.60}(AsF_{5.00})_{0.248}$. [d] Laboratory B. [e] Sample in footnote *d* analyzed 3 months later than the analysis given in the table: Ti = 1.73%; Al = 1.43%. [f] Empirical formula: $C_{7.00}H_{8.41}I_{0.225}$. Vacuum pumped; see Table VII.

yield. Below −38 °C essentially no film formation is observed. At 0 °C the film yield is quantitative. As the reaction temperature is increased from −38 to 0 °C decreasing amounts of soluble products form. Above 0 °C the yield drops somewhat to about 70% with the formation of some soluble material.

Note that the monomer temperature was also varied in these experiments in an attempt to maintain a constant rate of monomer vaporization, so that some of the observations may, in part, also result from this variable.

(3) Wash Solvent. Two wash solvents were primarily used: *n*-pentane and toluene. Toluene (or benzene) removed more material during washing than did pentane as graphically shown in Figure 2; the scanning electron micrographs show the result of dissolution of some of the pentane-washed film by toluene as observed visually by color in the toluene. More will be said concerning this effect in a later section. Use of a tetrahydrofuran/methanol (6/1) mixture did not yield a significantly different result in terms of film composition or behavior (see Table V).

(B) Molecular Structure. (1) Elemental Analyses. Table V displays the elemental analytical data for poly(1,6-heptadiyne) films. The expected C/H ratio for C_7H_8 is observed within experimental error. In spite of exhaustive washing procedures, ash was always present from the catalyst residues; pentane and toluene gave indistinguishable results in terms of ash content. Both Al and Ti were detected by energy dispersive X-ray analysis. The absolute values for percent C and percent H are not in agreement with calculated values. We believe this discrepancy is primarily due to the sensitivity of poly(1,6-heptadiyne) to oxidation (see section C below). Thus, unless the analyst rigorously excludes oxygen, poor analyses result; in fact, some commercial analytical laboratories routinely reported high oxygen content and concomitantly low carbon values. The fact that the samples, as prepared and sealed, contained no oxygen is borne out by results for doped analogues.

Table VI shows a comparison of analyses of undoped and doped films early in this work before the commercial analytical laboratories refined their handling techniques. Portions of a sample of poly(1,6-heptadiyne) film were sent to two different analytical laboratories. One found more than twice as much oxygen as the other! But when the same sample was doped with I_2 and AsF_5, neither analyst found oxygen. This comparison is taken as evidence for the introduction of oxygen into the undoped sample by the analysts. As Table V illustrates, this problem was largely overcome by improved techniques.

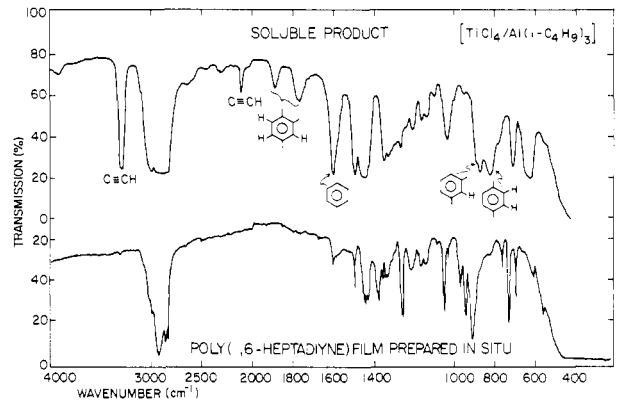

Figure 3. Infrared spectra of oligomeric 1,6-heptadiyne prepared with $TiCl_4/Al(i\text{-}C_4H_9)_3$ (top) and poly(1,6-heptadiyne) prepared with $Ti(OC_4H_9\text{-}n)_4/Al(C_2H_5)_3$ (bottom).

(2) Spectroscopic Studies. In addition to structures **2** and **3**, structures **4** and **5** are also possible for poly(1,6-heptadiyne). **2**, **4**, and **5** arise via different cyclopolymerization pathways.

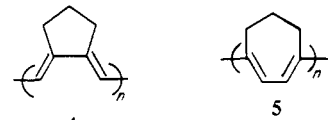

4 5

Poly-1,6 films upon heating in vacuo, e.g., 203 °C for 18 h, lose their metallic luster and become yellow-orange with no change in elemental composition; in thin samples the films become transparent. The soluble material prepared with the heterogeneous catalysts likewise was thermally unstable.[10] Presumably this transformation involves a double bond rearrangement, which eliminates the polyene backbone conjugation. The exo–endo double bond rearrangements of **2** to **6** and **4** to **7** and/or **8** are

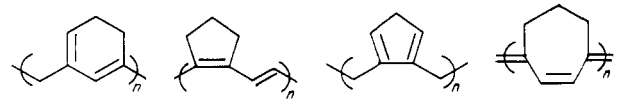

6 7 8 9

likely.[14] For **2** this would bring about loss of conjugation along the backbone; in the case of **4**, **8** would result in such loss also, but **7** might be more stable than **8**. **5** is presumably more stable than its isomer **9** and in either case backbone conjugation is maintained. On this basis structure **2** is favored and also in view of its stability and that associated with the transition state in the cyclopolymerization.

In order to address the possibility of structure **3**, 1,6-heptadiyne was oligomerized with a heterogeneous catalyst from $TiCl_4$ and $Al(i\text{-}C_4H_9)_3$. As reported,[12,13] the oligomeric material possessed infrared (IR) bands at 1890, 1780, 1600, 870, and 820 cm^{-1}, attributable to aromatic structures of type **3** (Figure 4). Unreacted acetylenic functionality was also detected (3300 and 2120 cm^{-1}). However, the free-standing films of poly(1,6-heptadiyne) do not possess these absorptions (Figure 3). Hence, structure **3** is not present to any detectable extent in films synthesized by using the homogeneous catalysts.

In order to differentiate between **2** and **4** spectroscopy was employed. A priori formation of the six-membered ring (**2**) was favored over that of the five-membered ring (**4**) as noted above. Therefore, model monomeric systems **10** and **11** were prepared

(14) P. DeMayo, "Molecular Rearrangements", Interscience, New York, 1963, Vol. 1, pp 40–42. R. Fuchs and L. A. Peacock, *J. Phys. Chem.*, **83**, 1975 (1979). R. B. Turner and R. H. Garner, *J. Am. Chem. Soc.*, **80**, 1424 (1958).

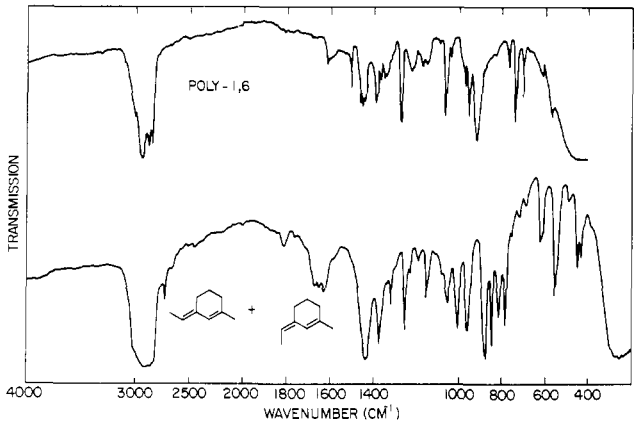

Figure 4. Infrared spectra of poly(1,6-heptadiyne) film (top) and mixture of *cis*- and *trans*-3-ethylidene-1-methylcyclohexane (**10** and **11**) (bottom).

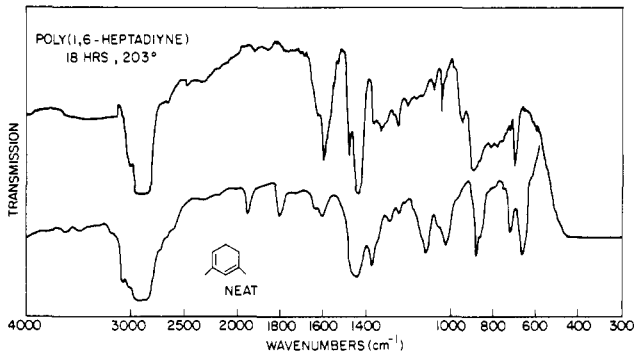

Figure 5. Infrared spectra of thermally treated (203 °C, 18 h) poly(1,6-heptadiyne) (top) and 1,3-dimethyl-1,3-cyclohexadiene (**13**) (bottom).

for comparison to poly-1,6. Figure 4 compares the IR spectra of a poly-1,6 film and of a mixture (80/20) of **10** and **11**. There

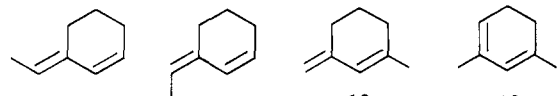

10 **11** **12** **13**

is an overall similarity, although some peaks appear to be shifted and there are others that are not common to both spectra. The greater simplicity of the polymer spectrum can, in part, be attributed to the fact that because the polymer is a solid there is greater damping and steric constraint of the chromophores in the polymer; this also may explain some of the shifts.

The infrared spectra of thermally rearranged poly-1,6 film and 1,3-dimethyl-1,3-cyclohexadiene (**13**), which results from thermal rearrangement of **12**, are compared in Figure 5. Again, the spectral changes are similar as are the resultant spectra, although minor peaks which occur in the monomeric diene in solution are absent in the corresponding polymeric solid. Thus, the infrared data on poly-1,6 and its rearrangement product support structure **2**.

In order to try to identify some of the IR bands in poly-1,6, 1,6-heptadiyne-*1,7-d*$_2$ was prepared and polymerized. The spectrum of the resultant polymer is compared to that of poly-1,6 in Figure 6. Clearly many shifts occur as expected. A few bands can be assigned with some confidence. The shoulders at 3020 and 3000 cm^{-1} are the =C—H stretches; these modes shift to 2230 and 2210 cm^{-1} upon deuteration (factors of 1.35 and 1.36). The 1600-cm^{-1} band is due to the polyene C–H out of plane vibration and appears to shift to 1185 cm^{-1} upon deuteration (factor of 1.35). The methylene scissor vibrations at 1420, 1435, and 1450 cm^{-1} are unaffected by deuteration of the terminal carbons of the monomer. The bands at 965, 940, and 910 cm^{-1} are attributed to the trisubstituted olefinic C–H out of plane vibrations; upon deuteration these appear to shift to 780, 730, and 695 cm^{-1} (factors

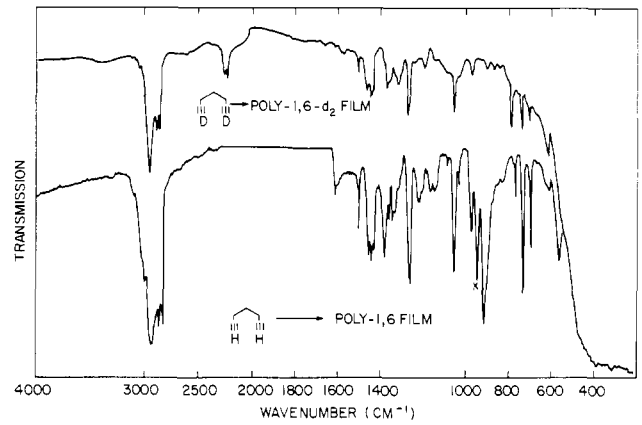

Figure 6. Infrared spectra of films of poly(1,6-heptadiyne-*1,7-d*$_2$) (top) and poly(1,6-heptadiyne) (bottom).

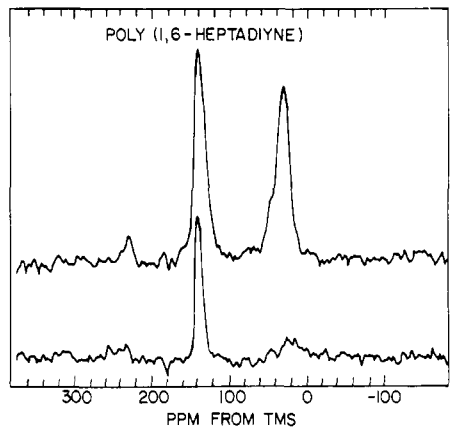

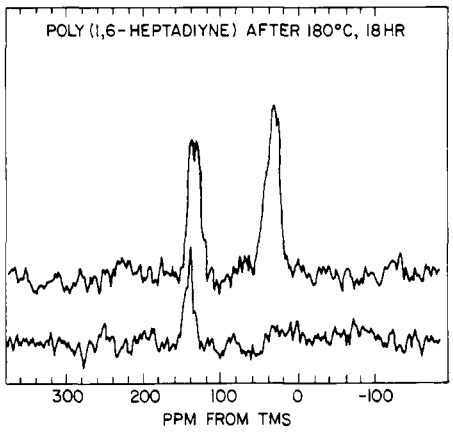

Figure 7. ^{13}C magic angle spinning–cross polarization NMR spectra, obtained at 22.63 MHz on a Bruker CXP spectrometer, of poly(1,6-heptadiyne) [top panel: full spectrum (top), nonprotonated carbon spectrum (bottom)] and thermally rearranged (180 °C, 18 h) poly(1,6-heptadiyne) [bottom panel: full spectrum (top), nonprotonated carbon spectrum (bottom)]. Repetition time = 1 s; cross polarization mixing time = 1 ms; ^{1}H decoupling power = 12 G; spin speed = 2.1 kHz. For the nonprotonated carbon spectra a 40-μs delay without radio-frequency power is inserted between the mixing and signal acquisition period.

of 1.24, 1.29, and 1.31). The trio of peaks at 760, 725, and 690 cm^{-1} in poly-1,6 may also be trisubstituted olefin C–H out of plane vibrations.

Magic angle spinning, cross polarization ^{13}C NMR spectra were recorded. Figure 7 shows the full ^{13}C spectrum and the delayed-decoupling nonprotonated ^{13}C spectrum[15] of poly-1,6, as

(15) S. J. Opella, M. H. Frey, and T. A. Cross, *J. Am. Soc.*, **101**, 5836 (1979).

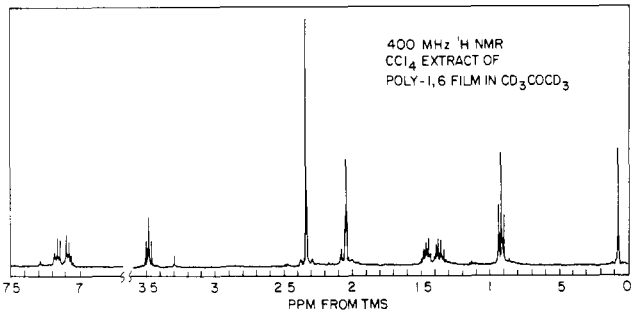

Figure 8. 400-MHz ^1H NMR spectrum of the CCl_4 extract of a poly(1,6-heptadiyne) film that had been exhaustively washed 12 months previously.

well as the corresponding spectra of the thermally rearranged poly-1,6. Consistent with the possible structures **2** and **4** for poly-1,6 and its thermally rearranged product, **6** or **8**, about half of the olefinic carbons are protonated ($\delta_c = 131 \pm 2$ ppm downfield from Me_4Si) and half nonprotonated ($\delta_c = 140 \pm 2$ ppm), and few quaternary aliphatic carbons are present. The rearranged product has at least two different olefinic carbons and two, or three, different aliphatic carbons.

In part F, below, it will be argued that a significant number of short chain segments are present in poly-1,6. The following results support this conclusion. After storage for several weeks or months poly-1,6 films (which had been rigorously washed upon synthesis) could be extracted with benzene or carbon tetrachloride to yield colored products. The proton NMR spectra of these materials are similar; the yellow CCl_4 extract's spectrum is shown in Figure 8. Exposure to air and room lights caused the solution to become dark purple. No further attempts were made to identify this material.

In view of the lack of solubility of the poly-1,6 films and the lack of crystallinity (see section D) and the solubility of films prepared with heterogeneous catalysts,[10] the polymer films must be cross-linked by moieties such as **14**. Such cross-links, of course, do not interrupt the backbone conjugation of the polymer.

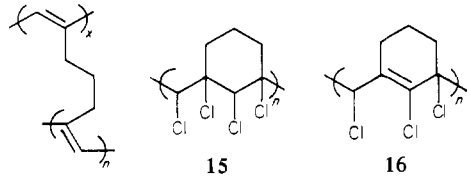

14

15 **16**

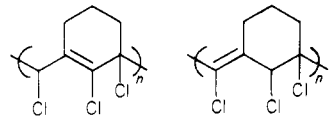

17 **18**

Chlorination of poly-1,6 caused the film to become nearly colorless and to more than double in weight. The soluble analog was reported by Stille and Frey[10] to take up nearly (91%) 2 mol of chlorine/monomer unit. In the present case the empirical formula is $C_7H_7Cl_3$. This result suggests that either chlorination was incomplete or that the solid polymer film of the expected tetrachloro derivative (**15**) eliminated HCl to form the trichloro derivative (**16**) and/or its isomers **17** and **18**. The product film does possess a C=C band at 1600 cm^{-1} and a C=C–H vibration at 920, the latter indicative of the presence of unreacted **2** or product **17**.

(3) Degeneracy of Polymeric Electronic Structure: Solitons. The structure **2** actually implies the existence of two equivalent bond structures for poly-1,6, **19a** and **19b**. These structures have

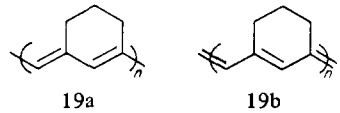

19a **19b**

equal energy and are equally probable, i.e., resonance forms. Regions of specific bond alternation, phase **19a** or **19b**, may occur within individual poly-1,6 chains. The interface or domain wall between regions of structure **19a** and structure **19b** contains a soliton defect (free radical), **19c**. These solitons[16,17] or domain

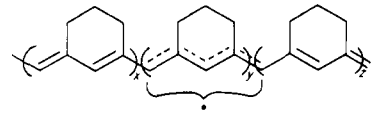

19c

wall defects[18] are similar to those postulated to occur in *trans*-polyacetylene.

For *trans*-polyacetylene, the domain wall is electrically neutral (i.e., a free radical) and is estimated[17] to be about 15 polyene carbons long. The neutral soliton (free radical) has an energy midway between the filled valence band and the empty conduction band and has a net spin[16-18] associated with it. The spin comes from the unpaired electron in the defect. When the soliton is charged (by adding or removing an electron from the bond alteration defect) to form an anion or a cation, it is spinless. Solitons may play an important role in the magnetic,[19,20] transport,[21-23] and optical[24] properties of polyacetylene.

It is seen below that solitons may have an important role in poly-1,6 as well, although the situation here is more complicated than in *trans*-polyacetylene. Though the two phases of bond alternation **19a** and **19b** have the same energy, three distinct radical structures **19d–f** are possible. **19d** and **19f** are very nearly

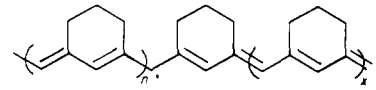

19d

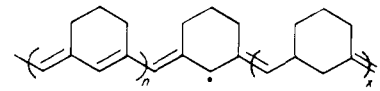

19e

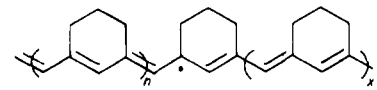

19f

identical secondary radicals but different in energy from **19e**, a degenerate tertiary radical. Hence this system is close to a realization of a linearly conjugated diatomic polymer, $(A{=}B)_x$. Soliton excitations have been proposed[24] for this latter case as well.

Solitons must be created in pairs. At low doping levels individual polarons (cation radicals) are created.[25] At higher concentrations two polarons may combine to form two solitons of

(16) M. J. Rice, *Phys. Lett.* **71A**, 152 (1979).
(17) W. P. Su, J. R. Schrieffer, and A. J. Heeger, *Phys. Rev. Lett.*, **42**, 1698 (1979); *Phys. Rev. B*, **22**, 2099 (1980).
(18) J. A. Pople and S. H. Walmsley, *Mol. Phys.*, **5**, 15 (1962).
(19) S. Ikehata, J. Kaufer, T. Woerner, A. Pron, M. A. Druy, A. Sivak, A. J. Heeger, and A. G. MacDiarmid, *Phys. Rev. Lett.*, **45**, 1123 (1980).
(20) A. J. Epstein, H. Rommelmann, M. A. Druy, A. J. Heeger, and A. G. MacDiarmid, *Solid State Commun.*, **38**, 683 (1981).
(21) A. J. Epstein, H. Rommelmann, M. Abkowitz, and H. W. Gibson, *Phys. Rev. Lett.*, **47**, 1549 (1981). A. J. Epstein, H. Rommelmann, M. Abkowitz, and H. W. Gibson, *Mol. Cryst. Liq. Cryst.*, **77**, 81 (1981).
(22) S. Kivelson, *Phys. Rev. B*, **25**, 3798 (1982).
(23) N. Suzuki, M. Ozaki, S. Etemad, A. J. Heeger, and A. G. MacDiarmid, *Phys. Rev. Lett.*, **45**, 1209 (1980). D. M. Hoffman, D. B. Tanner, A. J. Epstein, and H. W. Gibson, *Mol. Cryst. Liq. Cryst.*, **83**, 1175 (1982). D. M. Hoffman, H. W. Gibson, A. J. Epstein, and D. B. Tanner, *Phys. Rev. B*, **27**, 1454 (1983).
(24) M. J. Rice and E. J. Mele, *Phys. Rev. Lett.*, **49**, 1455 (1982).
(25) A. R. Bishop and D. K. Campbell in "Nonlinear Problems: Present and Future", A. R. Bishop, D. K. Campbell, and B. Nicolaenko, Eds., North Holland Publishing Co., Amsterdam, 1982, p 195. S. Etemad, A. Feldblum, A. J. Heeger, T. C. Chung, A. G. MacDiarmid, A. R. Bishop, D. K. Campbell, and K. Fesser, to be published.

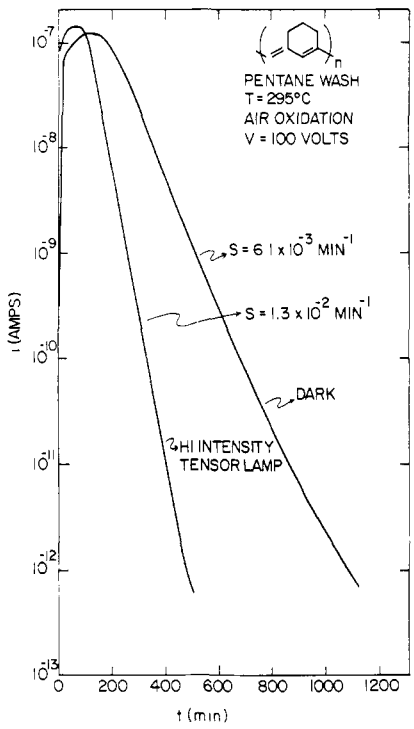

Figure 9. Change in conductivity upon exposure of poly(1,6-heptadiyne) film to oxygen.

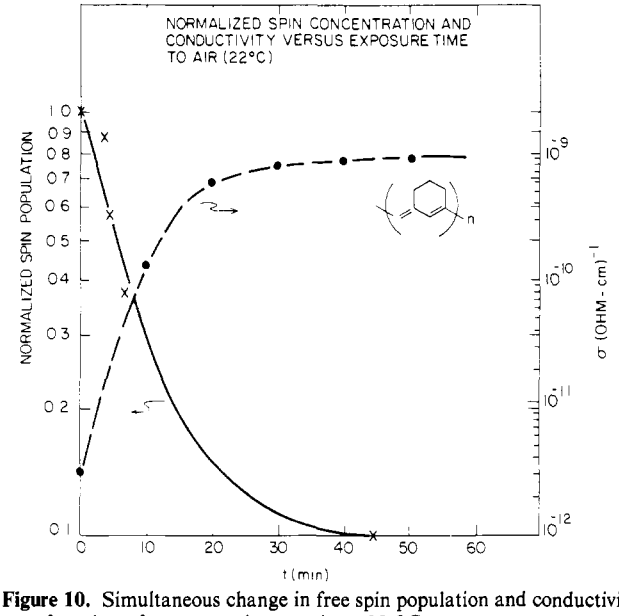

Figure 10. Simultaneous change in free spin population and conductivity as a function of exposure time to air at 22 °C.

lower energy. In order for this to occur, motion of the polaron along the polymer chain is necessary. This may be impeded in poly-1,6 due to the nondegeneracy (see section G below).

(C) Oxidation. Exposure of poly-1,6 to oxygen leads to two effects in sequence.[26] First, the oxygen dopes the polymer; the conductivity increases up to 4 orders of magnitude, as compared to the single order of magnitude observed with polyacetylene.[27] Second, the oxygen degrades the polyene, resulting in catastrophic loss of conductivity. These effects are exemplified in Figure 9. Note also the effect of light, as seen for polyacetylene,[27] in accelerating the oxidation.

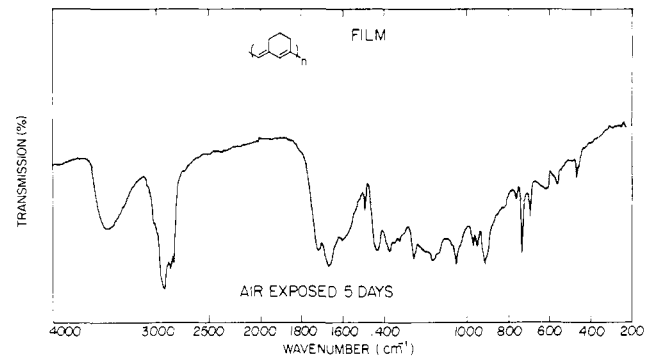

Figure 11. Infrared spectrum of a poly(1,6-heptadiyne) film after 5 days of exposure to ambient air.

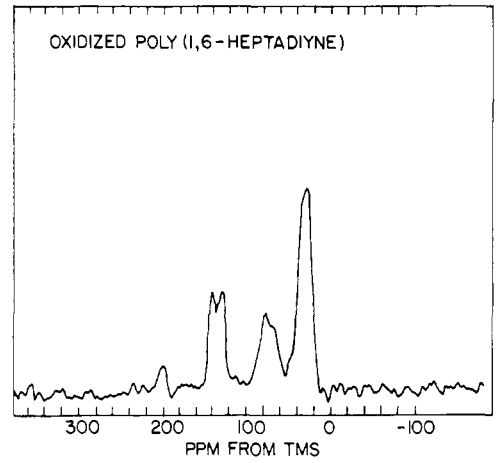

Figure 12. ^{13}C magic angle spinning–cross polarization spectrum of oxidized poly(1,6-heptadiyne) obtained at 22.63 MHz on a Bruker CXP spectrometer by using a 1-s repetition time, 1-ms cross polarization mixing time, 12-G ^1H decoupling, and 2.1-kHz spinning.

Unlike the situation described below for iodine doping, the number of free spins as detected by ESR during the doping by the weaker acceptor, triplet oxygen, *decreases*. As shown in Figure 10 a 10-fold decrease in spin population coincides with a 1000-fold increase in conductivity. This process presumably involves charge transfer of a free radical electron, a neutral soliton, from the polyene to oxygen, leading to a carbenium ion or "charged soliton", which is the active conductive species. Triplet oxygen, being a weaker acceptor than iodine, apparently cannot remove electrons from double bonds to form radical cations.

Slight differences in the rate of degradative oxidation of pentane (faster) and toluene (slower) washed samples were observed. However, the activation energies, 13 kcal/mol (0.6 eV), are identical and are similar to that of *trans*-polyacetylene, 13.8 kcal/mol (0.597 eV).[27] The overall rate of oxidation of poly-1,6 is more than 10 times as fast as that of polyacetylene. Treatment of poly-1,6 with a free radical quencher, Tinuvin 770, as described below, resulted in modest improvements in oxidative stability.[28]

Figure 11 is an infrared spectrum of a poly-1,6 film that had been exposed to ambient air for 5 days. As with polyacetylene,[27] oxidation results in the appearance of carbonyl peaks at 1680 and 1720 cm^{-1}, assigned to α,β-unsaturated and isolated chromophores,[29a] respectively, and a broad absorption at 3400 cm^{-1}, attributed to hydroxyl[29b] and hydroperoxy moieties.[30] Oxidation of poly-1,6 yields the ^{13}C NMR spectrum of Figure 12 where significant populations of carbonyls (δ_c = 200 ppm) and ether linkages (δ_c = 70 ppm) are detected.

(26) J. M. Pochan, D. F. Pochan, and H. W. Gibson, *Polymer*, **22**, 1367 (1981).
(27) H. W. Gibson and J. M. Pochan, *Macromolecules*, **15**, 242 (1982). J. M. Pochan, D. F. Pochan, H. Rommelmann, and H. W. Gibson, *Macromolecules*, **14**, 110 (1981).
(28) J. M. Pochan, H. W. Gibson, and J. Harbour, *Polymer*, **23**, 435 (1982).
(29) K. Nakanishi, "Infrared Absorption Spectroscopy", Holden-Day, San Francisco, 1962, (a) p 42, (b) p 30.
(30) N. A. Golub, *Pure Appl. Chem.*, **52**, 305 (1980).

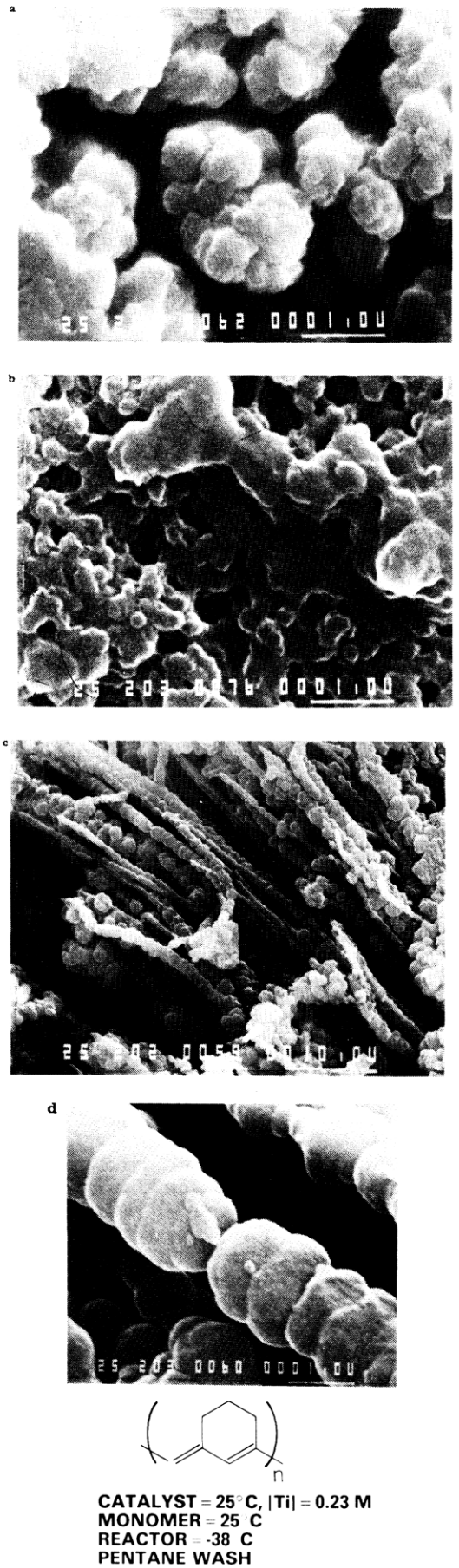

Figure 13. Scanning electron micrographs of poly(1,6-heptadiyne) films: (a) prepared at 20 °C; (b) prepared at 4 °C; (c) prepared at −38 °C; (d) prepared at −38 °C. Solid bars at lower right hand corners are 1.0, 1.0, 10, and 1.0 μm, respectively, in length.

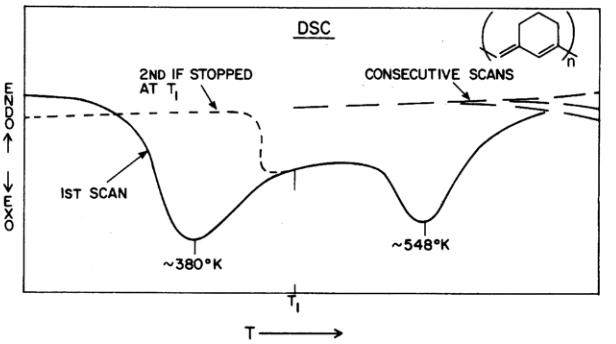

Figure 14. Differential scanning calorimetric (DSC) traces for poly(1,6-heptadiyne).

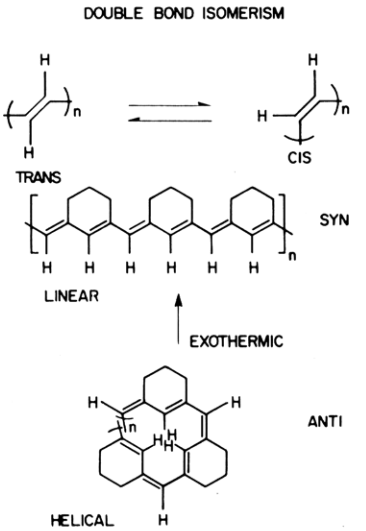

Figure 15. Helical and planar conformations of poly(1,6-heptadiyne).

(D) Solid-State Properties. The poly-1,6 film's solid-state structure was examined by a number of techniques. The density was estimated by film mass and measured dimensions to be 1.05 (±0.05) g/cm^3. This high density is consistent with the nonporous structure of the film.

Figure 13 presents morphological structures for the polymer films obtained as a function of reactor temperature. The morphology differs significantly from the fibrillar structure of $(—CH=CH—)_n$. Coalesced droplets (spheres) appear and the basic morphological structure varies as a function of the agglomeration of these spheres. The size of the individual spheres is smaller (1 μm) in films prepared at higher temperatures. The morphology thus is apparently controlled by the monomer vapor deposition rate. Fracture cross sections show the sample of Figure 13a to be almost free of voids and that of Figure 13b to be more porous. The agglomerated droplet fibrillar structure in Figure 13c,d is the most unusual morphology and explains the brittleness of films prepared at low temperatures. Because of this brittleness these samples could not be isolated as continuous films upon removal from the reactor vessel. The morphologies observed in Figure 13 are similar to those obtained for polypropylene at low and intermediate catalyst efficiencies.[31] At high catalyst efficiencies polypropylene exhibits a fibrillar morphology. A significant difference is that heterogeneous catalysis was used for polypropylene while in the present case a homogeneous catalyst was employed.

As seen in Figure 13c,d under certain conditions the polymer forms a "string of pearls" structure, "fibrils" being of ~1-μm diameter. Indeed, the central "string" portions are also observable in Figure 13c,d in some regions. The clumplike morphology seen

(31) J. Boor, Jr., "Ziegler-Natta Catalysts and Polymerizations", Academic Press, New York, NY, 1979. J. Wristers, *J. Polym. Sci., Polym. Phys. Ed.*, **11**, 1601 (1973).

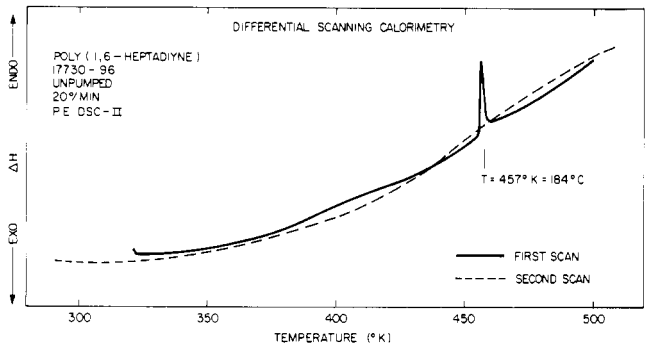

Figure 16. DSC trace at 20 °C/min for a sample of pentane-washed poly(1,6-heptadiyne) vacuum pumped for 4 days at 10^{-4} torr and then stored at 25 °C for 2 months.

in polyacetylene[32] is also observed in poly-1,6 as exemplified by certain regions of Figure 13c and in Figure 13a,b.

Differential scanning calorimetry (DSC) revealed two irreversible exothermic processes, one peaking at 107 °C and the other at 275 °C (Figure 14). The lower temperature process is attributed to rearrangement of the exo double bond of **2** to convert the polymer from a helical structure to a nearly planar polyene backbone configuration (Figure 15). This process may be compared to the isomerization of polyacetylene, for which a DSC exotherm is reported at 155 °C.[33] It is, therefore, believed that as made the films are mixtures of the two forms. All experiments were carried out on films stored at 25 °C under argon. The higher temperature process is attributed to the exo to endo rearrangement discussed above.

X-ray diffraction from the poly-1,6 films did not reveal any evidence of crystallinity. However, a vacuum-treated sample that had been washed with pentane possessed a sharp endotherm at 184 °C as shown in Figure 16. This endotherm might be due to a melting process. The same sample showed a broader endotherm when it was not vacuum treated. A toluene-washed sample that was vacuum pumped possessed an endotherm at 164 °C; a sample not vacuum treated did not possess this endotherm. Thin films of poly-1,6 are softened (plasticized) to a slight extent by toluene. It may, therefore, be that ordered domains exist but that they are very small. No electron diffraction experiments have been done on this polymer.

(E) Electrical Conductivity: Doping. Poly-1,6 films were doped with the acceptors iodine and arsenic pentafluoride. During the doping a series of visible color changes took place. With iodine the films changed from green to purple to blue to blue-black. With AsF_5 the change was from green to blue to blue-black. Figure 17 shows the kinetics for conductivity change upon I_2 doping at 25 °C in vacuo. Though sample to sample variations in the maximum conductivity value exist, the shapes of these curves are representative. The conductivity, σ, rises over about 1 h from the undoped level of 10^{-12} S/cm to a maximum value in the range 10^{-3}–10^{-1} S/cm and then decreases and plateaus at a lower level. Removal of the iodine source at the maximum decreases the conductivity loss past the maximum. Similar curves result from AsF_5 treatment. At room temperature the maximum conductivities observed were slightly less than 10^{-1} and 10^{-2} S/cm for I_2 and AsF_5 doping, respectively.

It is interesting to compare the kinetics of iodine doping of poly-1,6 with those of polyacetylene. Under the same conditions (25 °C, in vacuo) *trans*-polyacetylene reaches maximum conductivity in about 0.5 h,[34] changing by a factor of 10^6. As can

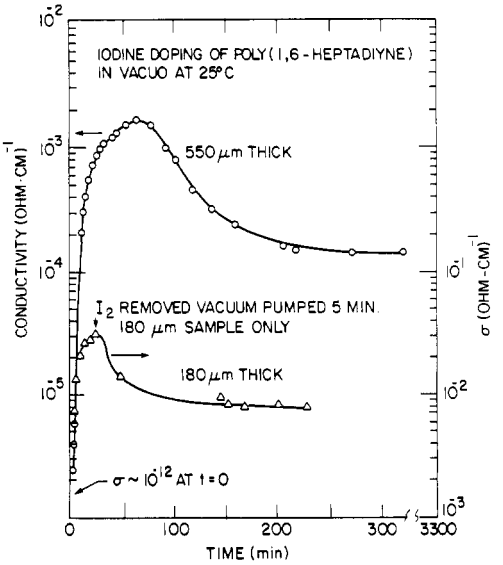

Figure 17. Conductivity of poly(1,6-heptadiyne) films as a function of time after exposure to iodine at 25 °C in vacuo.

Table VII. Comparison of Compositions of Fully Doped (25 °C) Poly(1,6-heptadiyne)(P-1,6), Polyacetylene (PAC),[2] and Poly(*p*-phenylene)(PPP)[2]

dopant species	equiv/double bond (conductivity, S/cm)		
	P-1,6	PAC	PPP
I[a]	0.50 (10^{-3}–10^{-1})	0.50[b] (10^{1})	*c*
I[d]	0.11 (10^{-4}–10^{-2})	0.30[b] (10^{-1}–10^{0})	*c*
	0.11[e] ($\leq 10^{-12}$)		
AsF_5[d]	0.11 (10^{-2})	0.28 (10^{2})	0.13 (10^{2})

[a] Without vacuum treatment. Equivalents on the basis of I atoms. [b] Starting with the cis isomer. [c] Iodine does not dope PPP. [d] Vacuum pumped; in the case of poly-1,6, 26 h, 25 °C, and 1×10^{-6} torr. [e] Thermally rearranged at 200 °C for 16 h prior to doping.

be seen from Figure 17 poly-1,6 changes by a factor of 10^6 over a period of 10 min. Thus, even though polyacetylene is porous, fibrous, and crystalline, while poly-1,6 is nonporous, continuous, and mostly amorphous, the normalized rates of charge of conductivity with doping are comparable. This will be discussed in section F in reference to ESR data as well.

Figure 18 shows the stability of iodine-doped poly-1,6 under argon and in ambient air. The conductivity under argon drops by a factor of 2 over 4 days but can be partially restored by reexposure to iodine. Thus, part of the conductivity loss can be attributed to loss of iodine or redistribution of the dopant in the film. When exposed to ambient air over a period of 17 days, the conductivity dropped by a factor of 10^4. Part of this drop may also be due to iodine loss or redistribution and part to oxidation.

In Table VII the compositions of the doped samples of poly-1,6 and rearranged poly-1,6 are compared to those of two other conducting polyenes, polyacetylene and poly(*p*-phenylene). It is interesting that the unpumped iodine contents of poly-1,6 and polyacetylene are similar, yet the latter retains about 3 times as much when pumped as does poly-1,6. Interestingly, the iodine content of the thermally rearranged poly-1,6 is the same as that of poly-1,6 although there is no rise in conductivity of the rearranged film. For AsF_5 dopant poly(*p*-phenylene) closely resembles poly-1,6.

While iodine is known to be present in polyacetylene as I_5^- or I_3^-, in agreement with the 40% loss with vacuum treatment (Table VII), the state of aggregation in poly-1,6 is not known. If I_3^- is the dopant species in the vacuum-pumped poly-1,6, then there

(32) H. Rommelmann, R. Fernquist, H. W. Gibson, A. J. Epstein, M. A. Druy, and T. Woerner, *Mol. Cryst. Liq. Cryst.* **77**, 177 (1981). A. J. Epstein, H. Rommelmann, R. Fernquist, H. W. Gibson, M. A. Druy, and T. Woerner, *Polymer*, **23**, 1211 (1982). The "String of pearls" type morphology that can be observed for polyacetylene is an artifact of evaporation of a thin layer of gold onto the polyacetylene surface (H. Rommelmann, R. Fernquist, A. J. Epstein, P. Bernier, M. Aldissi, and T. Woerner, *Polymer*, in press.

(33) T. Ito, H. Shirakawa, and S. Ikeda, *J. Polym. Sci., Polym. Chem. Ed.*, **13**, 1943 (1975).

(34) J. M. Pochan, H. W. Gibson, and J. Harbour, *Polymer*, **23**, 439 (1982). The $\sigma(T)$ of undoped *trans*-polyacetylene is better fit by a power law; see ref 21 and 22.

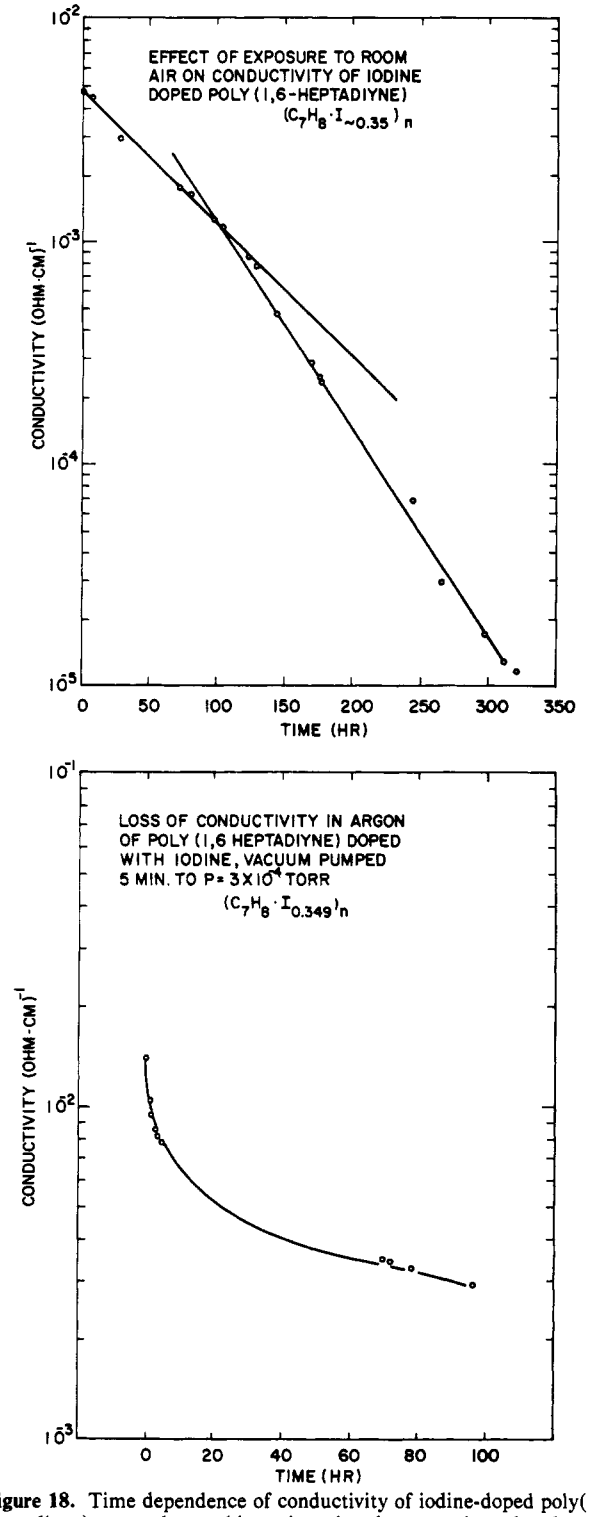

Figure 18. Time dependence of conductivity of iodine-doped poly(1,6-heptadiyne) exposed to ambient air and under argon in a closed vessel.

are only one-third as many "holes" (cations) in poly-1,6 as in polyacetylene. Assuming that the reduction in number of spins (as determined by ESR) in iodine-doped polyacetylene is a measure of the increase in the number of cations, the reported[34] decrease of spin population with increasing conductivity suggests that this factor of three difference in cation population will lower the conductivity of poly-1,6 by a factor of 10^{-2}–10^{-4} relative to polyacetylene. This expectation is borne out by the observed factor of 10^{-2}–10^{-5}. A similar factor of three in cation population is observed with AsF_5 doping and corresponds to a 10^{-4} factor in conductivity between poly-1,6 and polyacetylene. That this rationalization is oversimplified is shown by the fact that AsF_5-doped poly(*p*-phenylene), which has the same composition as AsF_5-doped

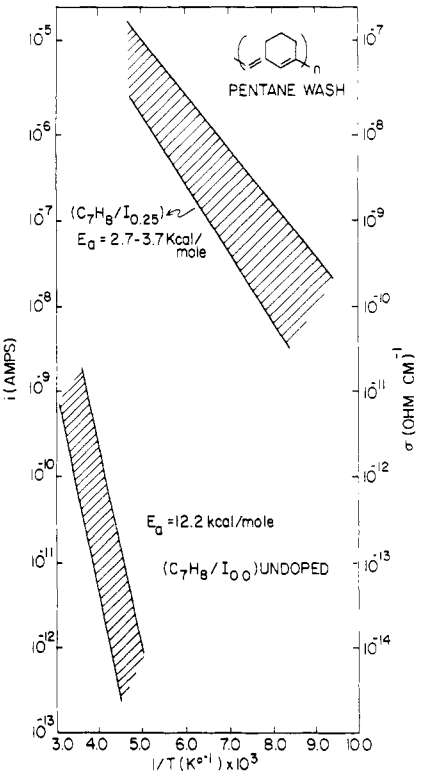

Figure 19. Generalized Arrhenius plots for conductivity of poly(1,6-heptadiyne) undoped and doped with iodine.

poly-1,6, has the same conductivity as AsF_5-doped polyacetylene. Obviously many other factors in addition to charge carrier concentration affect the conductivity, probably by affecting mobility.[2] Such factors could include molecular weight, crystallinity, steric interference between chains, etc.

The activation energy for conduction was derived from the temperature, T, dependence of conductivity. In Figure 19 are shown data covering a variety of samples that had been purified originally by using pentane as the wash solvent. As can be seen for the undoped films the activation energy is 12 kcal/mol (0.52 eV); similar values are seen for toluene-washed samples. For the iodine-doped samples the activation energy is 3–4 kcal/mol (0.1–0.2 eV). These values may be compared to activation energies of 8.7 kcal/mol (0.38 eV) (below 25 °C) and 16.0 kcal/mol (0.693 eV) (above 25 °C) for undoped[34] and 1 kcal/mol (0.04 eV) for iodine-doped[35] *trans*-polyacetylene. Thus, the apparent activation barriers in the two systems are comparable, despite the differences in molecular and solid-state structures.

Most conductivity–temperature experiments on poly-1,6 were conducted below 303 K because of possible molecular rearrangement (see above). When these measurements were done at constant voltage in a scanning temperature mode at 1 °C/min, a change in slope, sometimes accompanied by a current maximum, was observed in the temperature region 250–275 K (see Figure 20). This latter effect is generally associated with a molecular relaxation[36] and may correlate with NMR relaxation (see below). The apparent activation energy for transport increases above the 250–275 K temperature region, while for polyacetylene such a change occurs at 298 K. Since planar electronic structure is thought to enhance bond alternation and extended conjugation, any molecular relaxation that perturbed this structure would increase the activation energy for transport.

(35) C. K. Chiang, Y. W. Park, A. J. Heeger, H. Shirakawa, E. J. Louis, and A. G. MacDiarmid, *J. Chem. Phys.*, **69**, 5098 (1978). For heavily iodine doped polyacetylene, the conductivity is better fit by other functional forms such as $\sigma\alpha \exp(-T_0/T)^{1/4}$ with T_0 constant [A. J. Epstein, H. W. Gibson, P. M. Chaikin, W. G. Clark, and G. Gruner, *Phys. Rev. Lett.*, **45**, 1730 (1980); *Chim. Scripta*, **17**, 135 (1981)].

(36) J. VanTurnhout, "Thermally Stimulated Discharge of Polymer Electrets", Elsevier Scientific Publishing Co., New York, 1975.

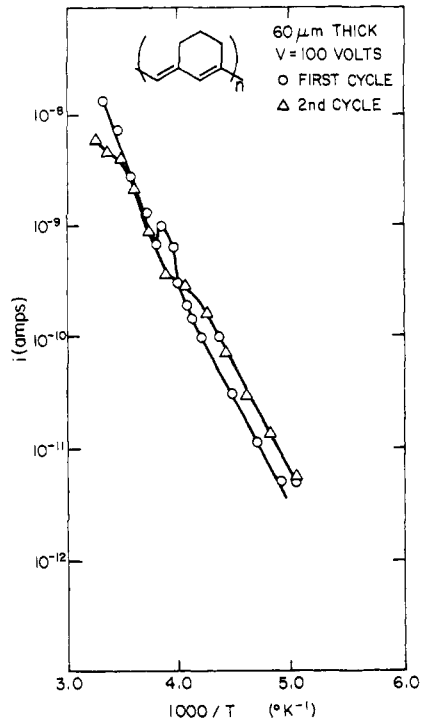

Figure 20. Current–reciprocal temperature relationship for a poly(1,6-heptadiyne) film. Temperature raised at 1 °C/min. Note current maximum at $1/T = 4.0 \times 10^{-3}$ K.

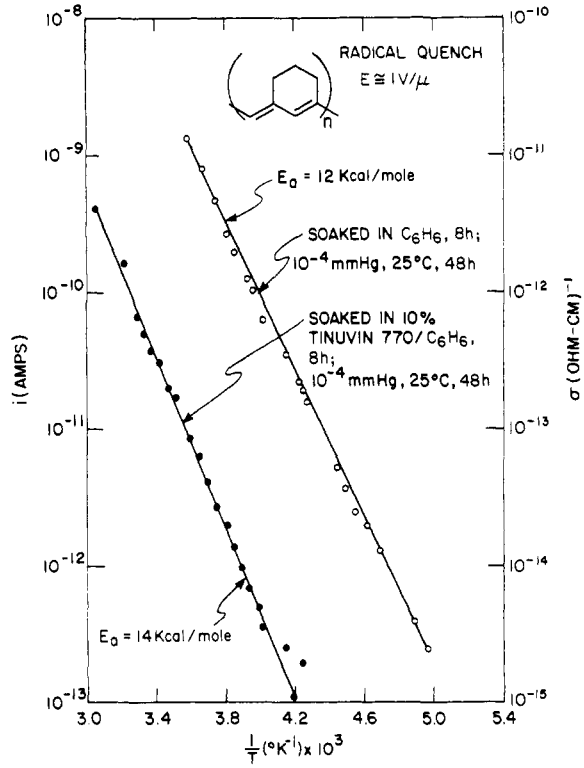

Figure 21. Arrhenius plots for conductivity of poly(1,6-heptadiyne) treated with Tinuvin.

Some interesting observations were made when poly-1,6 was treated with a free radical quencher, Tinuvin 770, whose partial structure is **20**.[28] As shown in Figure 21 two features result: (1)

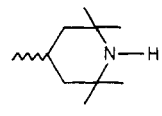

20

Scheme I

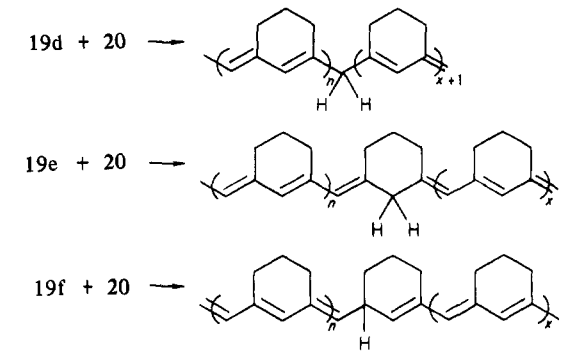

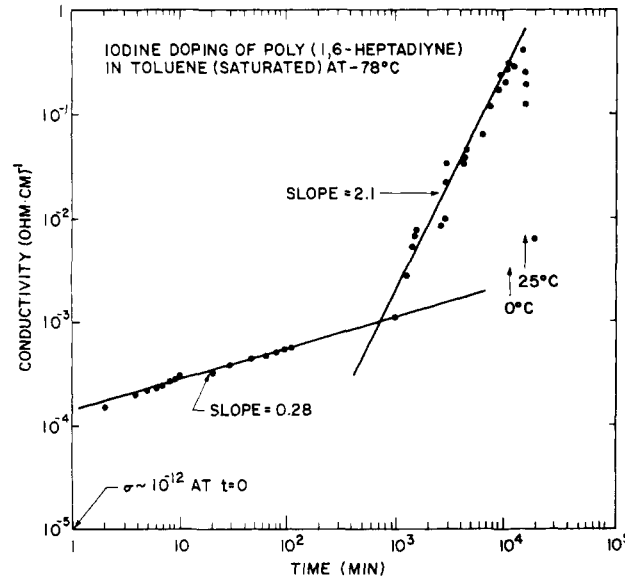

Figure 22. Conductivity of poly(1,6-heptadiyne) film as a function of exposure time to an iodine-saturated toluene solution at −78 °C.

the conductivity of the undoped polymer (pentane or toluene washed) decreases by a factor of 10^{-2} at constant temperature and (2) the activation energy (E_a) is unchanged within the limits of error (±2 kcal/mol). Further examination of the activation energy for conductivity has shown that contrary to Figure 3 of our earlier paper,[28] pentane- and toluene-washed samples yield comparable values of E_a before and after Tinuvin treatment. The decrease in conductivity can be rationalized as being due to an interruption of the conjugated backbone by hydrogen atom transfer from the Tinuvin, i.e., Scheme I; this would reduce the charge carrier mobility.

In view of the above-noted thermal rearrangement of the exo double bond to the endo position, the maximum in conductivity upon doping of poly-1,6 was believed to be due to dopant-catalyzed chemical rearrangement. To circumvent this problem, the doping was carried out at low temperature. Figure 22 shows log (conductivity) as a function of doping time (logarithmic scale) at −78 °C using a saturated solution of iodine in toluene. This process led to a conductivity of 0.4 S/cm, but required 1 week; the conductivity was still increasing at this point. Immediately upon raising the temperature to 0 or 25 °C the conductivity began to decrease. By reference to Figure 19 it can be seen that the conductivity of iodine-doped poly-1,6 is 10 times as great at 25 °C as at −78 °C ($1/T = 5.13 \times 10^{-3}$). On this basis, in the absence of chemical rearrangement, the value of >0.4 S/cm at −78 °C translates to >4 S/cm at 25 °C. Thus, poly-1,6 could in the absence of chemical rearrangement be doped to about the same level of conductivity as polyacetylene, in spite of the differences in molecular and solid-state structures.

(F) Magnetic Properties. Both ESR and magnetic susceptibility measurements have been carried out on poly-1,6. The ESR spectrum reveals a g value (2.0026) very similar to that of po-

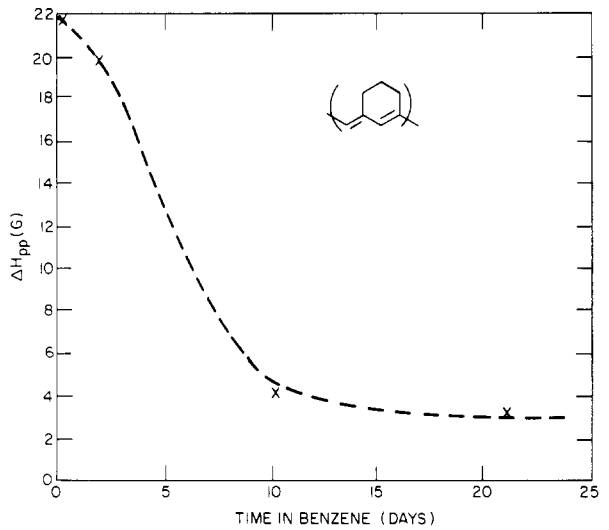

Figure 23. ESR line width of poly(1,6-heptadiyne) vs. soaking time in benzene.

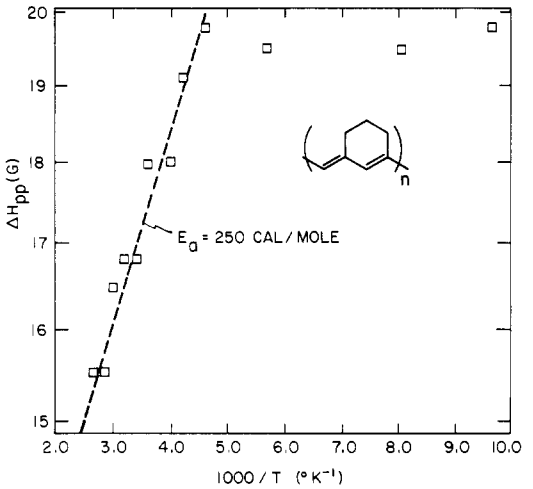

Figure 24. Temperature dependence of ESR peak to peak line width (ΔH_{pp}) of poly(1,6-heptadiyne) film.

lyacetylene (2.0023), but the line width (ΔH) is about 10 times larger for poly-1,6. The line width, however, is a function of the extent of washing and the time after washing. This effect is graphically shown in Figure 23; the line width decreases from 22 to 3 G after soaking 3 weeks in benzene. This treatment is believed to extract low molecular weight chains from the film and perhaps induce crystallization (see section B). Due to their shorter conjugation lengths any radicals on these chains would show large ΔH values relative to those on more delocalized higher molecular weight chains. The limiting 3-G line width may be compared to 0.8 G for *trans*-polyacetylene. The difference may be due to shorter conjugation lengths or to the fact that the various radical structures (**19d–f**) have different energies, thus limiting delocalization. The ESR spectrum of the polymer prepared from 1,6-heptadiyne-*1,7-d*$_2$, which presumably contains deuterium atoms on the backbone carbons, also has a line width, ΔH_{pp}, of 20 G at room temperature but appears to be Gaussian.

The temperature dependence of the ESR line width of poly-1,6 is shown in Figure 24. The linewidth varies between 220 and 365 K. The apparent activation energy is 0.25 kcal/mol (0.01 eV), a value very similar to that observed for polyacetylene within this temperature region.[37] More important, below 220 K ΔH becomes temperature independent. This temperature correlates with changes in activation energy of conductivity and a solid-state relaxation in the proton NMR.

(37) H. W. Gibson, J. Harbour, and J. M. Pochan, to be published.

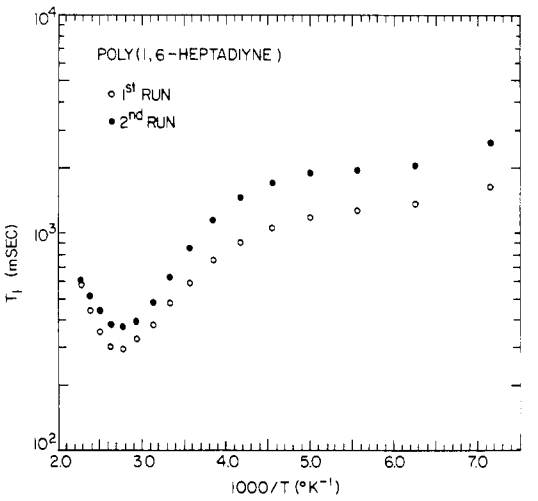

Figure 25. Temperature dependence of the spin–lattice relaxation time in poly-1,6 measured by the 180–*T*–90 sequence at 90 MHz on a Bruker CXP spectrometer. For each run measurements were made by increasing the temperature from 140 to 440 K.

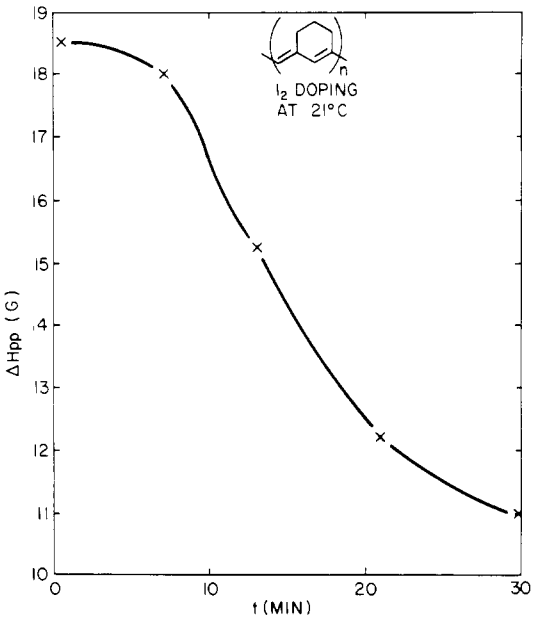

Figure 26. Line width (ΔH_{pp}) of poly(1,6-heptadiyne) as a function of iodine exposure time in situ in an ESR spectrometer. Relative intensity increased only slightly during the experiment.

Proton NMR spin–spin (T_2) and spin–lattice (T_1) relaxation measurements at 90 MHz were taken as a function of temperature from 140 to 440 K. The spin–spin relaxation behavior shows no anomalies, with T_2 changing gradually from 10 ms at 140 K to 14 ms at 440 K. Spin–lattice relaxation, however, shown in Figure 25, displays a minimum centered at ca. 365 K and is temperature independent below 220 K. In the absence of a T_2 transition we attribute the T_1 minimum to the effect of spin diffusion to spin sites, e.g., mobile side or end groups, with sufficient molecular motion to induce relaxation. Aside from the slight shift toward longer T_1 values after the first run, the T_1 behavior is reversible and appears to correspond to the same molecular process responsible for the change in ESR line width and the current maximum in the first-cycle conductivity measurements. Note also that the shape of Figure 25 mimics that of Figure 24 for $1/T > 2.5 \times 10^{-3}$.

Iodine doping decreases the line width (ΔH_{pp}) of poly-1,6 as shown in Figure 26. This decrease is in contrast to the results for polyacetylene; no change in line width is observed.[34] This result is consistent with the suggestion that short polymer radicals are present in the sample. These more localized radicals would be

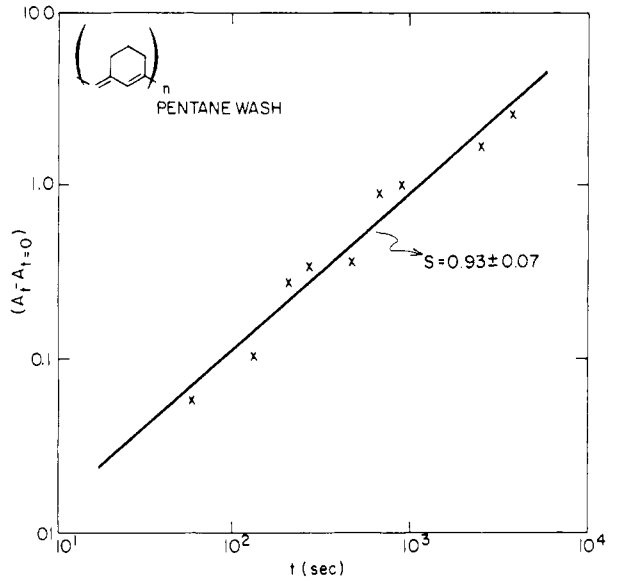

Figure 27. Relative spin population of poly(1,6-heptadiyne) as a function of exposure time to iodine at 25 °C in vacuo.

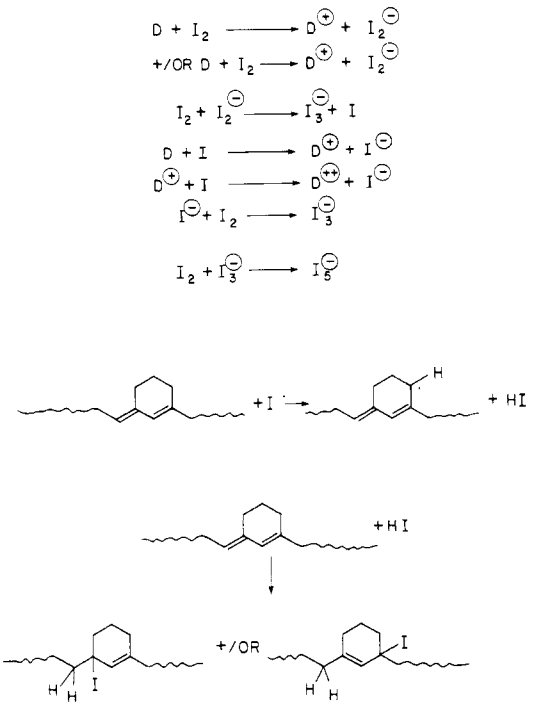

Figure 28. Possible scheme for interaction of iodine and poly(1,6-heptadiyne).

of higher energy than longer polyene radicals and would yield broad lines. Thus, the localized free radical electrons could be selectively removed by the acceptor (iodine), resulting in decreased line width.

The radical population of poly-1,6 *increases* upon doping with iodine, in contrast to that of polyacetylene.[34] The time dependence of this spin increase as measured in situ by ESR is shown in Figure 27. The log–log plot has a slope of 1. This slope is inconsistent with a completely diffusion controlled process;[38] instead it indicates a first-order process, interaction of I_2 with the free radicals. There are two possibilities: (1) the electron transfer process occurs on the surface of the poly-1,6, followed by diffusion of the cations and I_3^- and I_5^- ions into the bulk (more likely) or (2) the electron-transfer process occurs in the bulk but at a rate slower than the diffusion rate of iodine molecules through the film (less likely).

(38) P. V. Danckwerts, *Trans. Faraday Soc.*, **46**, 300 (1950).

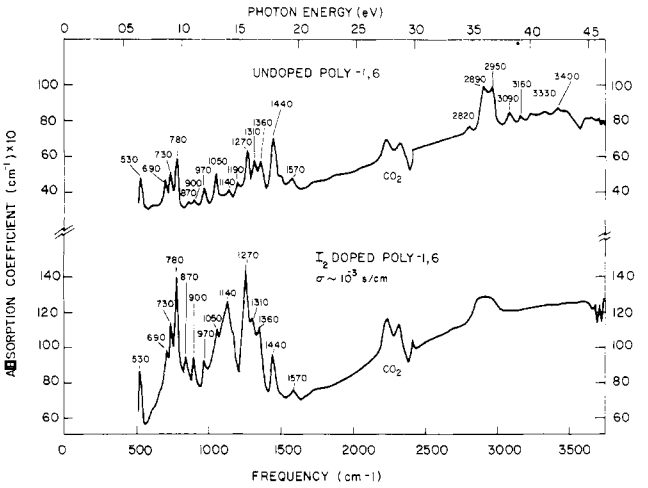

Figure 29. Infrared spectra of poly-1,6 (top) and I_2-doped poly-1,6 (bottom).

The increase in free radical population of poly-1,6 upon doping can be rationalized by one of two pathways given in the sequence of reactions in Figure 28. First, the doping mechanisms could in part entail electron transfer from a π-electron of a double bond (denoted by D for donor) to I_2 to yield a cation radical ($D^{+\cdot}$), thereby increasing the radical population. Second, as suggested for polyacetylene,[2,6] the doping process could involve removal of the higher energy electrons associated with free radicals ($D^{\cdot}$), but iodine radicals generated in the process could abstract the labile allylic hydrogen atoms. Addition of the resultant HI to double bonds could disrupt the polyene conjugation, leading to the conductivity maximum at 25 °C as discussed above. Thus, poly-1,6 may differ from polyacetylene only in this side reaction. In fact, at long doping times with iodine a maximum is seen in the conductivity of polyacetylene[34] and the spin population increases;[39] this may be due to a similar sequence of reactions involving the allylic hydrogen atoms present at cross-link sites.[40] While we believe the second mechanism may be operative, we favor the former explanation coupled with the persistence of the radical cations (see section G).

(G) Infrared and Optical Properties. The infrared absorption coefficients of poly(1,6-heptadiyne) and I_2-doped poly(1,6-heptadiyne) are shown in Figure 29. The frequencies of the sharp vibrational features are essentially the same in both the undoped and the doped material. Doping induces three broad features at 750, 1100, and 1300 cm^{-1}. In polyacetylene, doping-induced vibrational peaks occur at 900 and 1370 cm^{-1} while in $(CD)_x$ there are three lines at 790, 1160, and 1270 cm^{-1}.

At frequencies above 4000 cm^{-1}, the absorption coefficient is large enough that the 40 μm thick films are almost opaque. (*trans*-Polyacetylene films of similar thickness also become opaque around 4000 cm^{-1}.) At higher frequencies, the optical reflection was measured. Figure 30 shows the reflectance of a poly-1,6 film (shiny side) from the infrared to the ultraviolet. The reflectance has a large peak at 2 eV (16 000 cm^{-1}) with a shoulder at 1.5 eV (12 000 cm^{-1}). There is a minimum in the reflectance at 3.2 eV (26 000 cm^{-1}). This reflectance is quite similar to the spectrum of *trans*-polyacetylene, where there is a reflectance maximum near 1.9 eV,[6,41] which arises from an interband (valence to conduction) transition.

The reflectance spectrum of iodine-doped poly-1,6 is shown in Figure 30. Doping induces new vibrational structure in the in-

(39) P. Bernier, M. Rolland, M. Galtier, A. Montaner, M. Regis, M. Candille, C. Benoit, M. Aldissi, C. Linaya, F. Schue, J. Sledz, J. M. Fabre, and L. Giral, *J. Phys. Lett.*, **40**, L-297 (1979).

(40) V. Enkelmann, W. Muller, and G. Wegner, *Syn. Met.*, **1**, 185 (1980). J. C. W. Chien, *J. Polym. Sci., Polym. Chem. Ed.*, **19**, 249 (1981).

(41) A. Feldblum, J. H. Kaufman, S. Etemad, A. J. Heeger, T.-C. Chung, and A. G. MacDiarmid, *Phys. Rev. B*, **26**, 815 (1982). C. R. Fincher, Jr., D. L. Peebles, A. J. Heeger, M. A. Druy, Y. Matsamura, A. G. MacDiarmid, H. Shirakawa, and S. Ikeda, *Solid State Commun.*, **27**, 489 (1978).

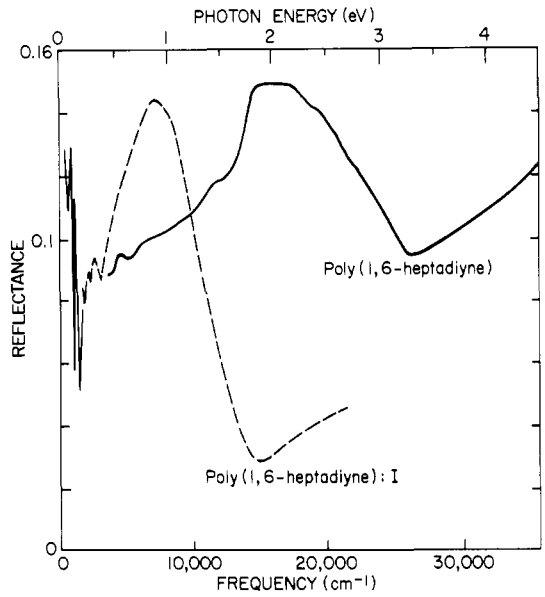

Figure 30. Far-infrared to ultraviolet reflectance spectra of undoped poly(1,6-heptadiyne) film (solid curve) and iodine-doped (saturated) poly(1,6-heptadiyne) film (dashed curve).

frared (as seen in Figure 29) and leads to a strong reflectance peak centered near 0.9 eV (7200 cm^{-1}). The original 2-eV peak of the undoped material is absent. The energy of the 0.9-eV peak is close to the 0.8-eV energy of a doping-induced absorption peak in *trans*-polyacetylene.

In *trans*-polyacetylene this "midgap absorption" has been attributed to an electronic transition from the valence band to a positive soliton (a domain wall or delocalized carbenium cation).[6,16-18] The positive soliton occurs when the dopant molecule accepts an electron from a neutral soliton (or free radical) state which lies midway between the valence and conduction bands. Within the soliton model the doping-induced infrared absorption at lower frequencies arises from localized vibrational modes of the soliton. This soliton model is consistent with the decrease in the number of free radicals during the doping of polyacetylene.[34,42] In contrast, as described in part F above, the number of free radicals (or neutral solitons) in poly-1,6 *increases* during doping. This increase makes it likely that the 0.9-eV peak in the reflectance spectrum of doped poly-1,6 is not due to a transition to a midgap soliton state. Instead, the absorption probably results from a radical cation state, as proposed in Figure 28. Recent calculations for polyacetylene indicate such a situation will lead to two "polaron" levels, one 0.4 eV above the midgap and one 0.4 eV below.[43] Assuming the energetics in poly-1,6 are similar, the 0.9-eV absorption in iodine-doped poly-1,6 can be attributed to a transition from the lower singly occupied radical cation (polaron) energy level to the upper empty level.

The difference in behavior of poly-1,6 and polyacetylene upon doping can be rationalized in terms of molecular structure. Two polarons in polyacetylene can annihilate to a pair of cations (positive solitons) with formation of a new bond:

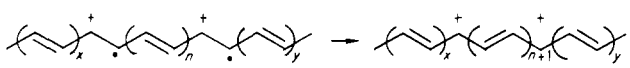

This is due to the degeneracy of the structure of polyacetylene; the free radical electron and the cation can interchange positions on adjacent carbon atoms with no cost in energy. In poly-1,6 this is not the case. Because of the presence of the alkyl substituent on every other carbon atom, the cation may prefer to reside on the tertiary carbon rather than on the secondary carbon to a greater extent than the free radical, i.e.

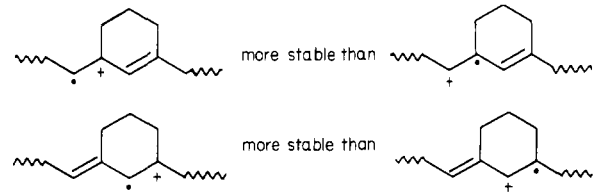

This preference will lead to the formation of structures such as

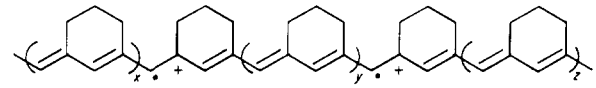

and introduce energy barriers to the transformation of two polarons (radical cations) into a re-formed bond and two cations, i.e., form two charged solitons. Hence, a fraction of polarons (radical cations) will persist in the sample upon doping, thereby increasing the total radical population. The process of polaron formation (by removal of an electron from a double bond) and persistence must predominate over the removal of a free radical electron (neutral soliton) in view of the increase in spin population during doping.

Conclusions

The present work demonstrates that cyclopolymerization enables the synthesis of substituted polyacetylenes, which are otherwise formed only with difficulty. The cyclopolymer poly(1,6-heptadiyne) can be prepared as free-standing films by using homogeneous Ziegler-Natta catalysts. The molecular structure of the film is indicated to be the six-membered ring structure on the basis of model compound IR studies and ^{13}C NMR spectra. The films are dense and continuous, in contrast to the porous structure of polyacetylene; poly-1,6 appears to be nearly completely amorphous, again in contrast to the 80–90% crystallinity of polyacetylene.[44,45] Poly-1,6 is more susceptible to oxidation than polyacetylene; however, unlike the latter it can be stabilized to moderate extent by treatment with antioxidant solutions.

In spite of these differences in molecular and solid-state properties compared to those of the prototypical polyacetylene, poly-1,6 can be doped to high conductivity, 0.1 and 0.4 S/cm at 25 and −78 °C, respectively. Moreover, the kinetics of doping of poly-1,6 are comparable to that of polyacetylene as measured by changes in conductivity and ESR signal. Poly-1,6 appears to retain about $^1/_3$ as much dopant upon vacuum treatment as polyacetylene, consistent with its lower conductivity; the activation energy of doped poly-1,6 is also higher by a factor of 3. In contrast to the behavior of polyacetylene, the doping of poly-1,6 is accompanied by an increase in the number of spins (free radicals). This result suggests that polarons (radical ions) are stable in poly-1,6, whereas they annihilate in polyacetylene; such polarons are consistent with the asymmetric nature of the molecular structure of poly-1,6. These results are not inconsistent with the optical band gap change upon doping (2 to 0.9 eV; cf. 1.9 to 0.8 for polyacetylene).

In summary, we have reported the synthesis, doping, and characterization of free-standing films of a substituted polyacetylene. Poly-1,6 affords many contrasts to polyacetylene in molecular and solid-state structures yet behaves similarly in terms of doping kinetics and conductivity. In the present work we have shown that a polymer that is amorphous, at least on the X-ray scale, has low surface area and porosity and probably has a significant portion of short conjugation lengths can be doped to high conductivity. Similarly, polyacetylene prepared by extrusion from a precursor polymer has short chains, high density, and low surface

(42) A. J. Heeger and A. G. MacDiarmid, *Chim. Scr.*, **17**, 115 (1981).
(43) A. R. Bishop, D. K. Campbell, and K. Fesser, *Mol. Cryst. Liq. Cryst.*, **77**, 253 (1981). J. L. Bredas, R. R. Chance, and R. Sibley, *Polym. Prepr., Am. Chem. Soc., Div. Polym. Chem.*, **23** (1), 82 (1982). J. P. Albert, C. Jouanin, and P. Bernier, *Polym. Prepr., Am. Chem. Soc., Div. Polym. Chem.*, **23** (1), 84 (1982).
(44) T. Akaishi, K. Miyasaka, K. Ishikawa, H. Shirakawa, and S. Ikeda, *J. Polym. Sci., Polym. Phys. Ed.*, **18**, 745 (1980).
(45) P. Robin, J. Pouget, R. Comes, H. W. Gibson, and A. J. Epstein, *Phys. Rev. B*, **27**, 3938 (1983).

area and is amorphous but can be doped to high conductivity.[46] Similarly polypyrrole is ordered only on a very small scale observable only by electron diffraction, and yet it too is highly conductive.[47] These results call into question some of the conclusions regarding prerequisites for high electrical conductivity in conjugated polyenes (crystallinity, long conjugation lengths, high surface area, i.e., porosity) as well as the underlying mechanism(s) of the transport process.

Experimental Section

General. All glassware was washed with aqua regia, deionized water, and acetone and oven-dried (110 °C) prior to use. Prepurified grade argon for Schlenk tube operations was scrubbed to an oxygen level of <0.8 ppm and water level of <5 ppm by using a modified Ace-Burlitch setup by passage through an oxygen getter and molecular sieves. A Vacuum Atmospheres HE series glovebox was maintained at <0.8 ppm of oxygen (Westinghouse Hagan meter) and <0.4 ppm of water (Vacuum Atmospheres Moisture Analyzer AM-2). The vacuum systems employed oil diffusion pumps backed by mechanical rough pumps and were capable of 10^{-6} torr. Spectrograde toluene was dried by reflux over sodium and then distilled under argon directly into a vessel attachable to the vacuum line; prior to attachment of the vessel to the vacuum line triethylaluminum was added to ensure dryness. Benzene was similarly purified. Similarly, spectrograde pentane was dried over P_2O_5 and then sodium. Tetrahydrofuran (spectrograde) was dried over sodium just prior to use. Methanol was dried over and distilled from Mg metal under argon. All solvents were degassed just prior to use on the vacuum line by application of at least six freeze–thaw cycles. Solutions (25%) of tri(isobutyl)aluminum and triethylaluminum in toluene (Aldrich) and triethylaluminum and trimethylaluminum in hexane (Aldrich) were used as received. Titanium tetra(*n*-butoxide) (Ventron, Alfa) was purified by distillation (bp 183.5 °C/8.2 torr) under argon; titanium tetra(isopropoxide) (Ventron, Alfa) was similarly treated (bp 77 °C/0.50 torr). Titanium tetra(*n*-nonylate) (Ventron, Alfa) was used as received. 1,6-Heptadiyne (Columbia Organic Chemicals) was purified by distillation (bp 104.0 °C) under argon through an adiabatic 75-plate Teflon spinning band apparatus (Nester-Faust-51); it was also degassed by freeze–thaw cycling at least 6 times on the vacuum line just prior to use. Elemental analyses were carried out by the Spang Microanalytical Laboratory, Eagle Harbor, MI, and Galbraith Laboratories, Knoxville, TN. Except where noted, all polymer samples were handled in the absence of oxygen and water by use of vacuum line, Schlenk tube, and glovebox techniques. Samples for elemental or other analyses were sealed in appropriate containers under vacuum or argon.

Instrumentation. Infrared spectra of Figures 3–6 and 11 were recorded on a Perkin-Elmer 283 instrument in demountable cells consisting of the polymer film sealed between KBr plates under argon or sealed solution cells. With a home-built grating spectrometer[48] infrared absorption spectra and infrared–ultraviolet reflectance spectra of the polymer films (Figures 29 and 30) were recorded. Solution-phase carbon and proton NMR spectra were determined on a Bruker WP-80 instrument. Solid-state NMR spectra (T_1, T_2, ^{13}C magic angle) were obtained by use of a Bruker CXP instrument. ESR measurements were taken on a Varian E-109 operating at a frequency of 9.5 GHz and power levels of 1–10 MW. A Perkin-Elmer DSC-II was utilized to gather the thermal data. Scanning electron micrographs were recorded on Jeolco JSM-35 instrument. Conductivities were measured in a two-probe mode either by use of Electrodag conductive adhesive bound platinum wires attached to a Simpson Model 461 digital multimeter or by direct pressure contacts (ohmic) to the top and bottom surfaces of the films in series with a Keithly regulated voltage supply and a Keithly 616 electrometer. Four-probe measurements were made by using Electrodag conductive adhesive bound platinum wires and a General Radio bridge setup or Electrodag conductive adhesive bound to gold wires in a Lakeshore Cryotronics closed cycle refrigerator.

1,6-Heptadiyne-*1,7-d*$_2$. To a stirred solution of 100 mL (0.120 mol) of 1.3 M methyllithium in ether (Ventron, Alfa) at −20 °C under argon was added 5.06 g (0.110 equiv) of 1,6-heptadiyne dropwise over 10 min. After 30 min 4.0 mL (0.222 equiv) of D_2O (99.8%, Aldrich) was added. The mixture was allowed to come to room temperature and diluted with 25 mL of H_2O to dissolve the LiOH formed. From the ether layer was isolated by spinning band distillation the desired product, bp 103.0–103.5 °C. Proton NMR ($CDCl_3$) showed loss of a triplet (J = 2.5 Hz) at δ 1.97 (H—C≡C) and simplification of the triplet of doublets (J = 2.5, 6.5 Hz) at δ 2.3 (C≡C–CH_2–) in the starting material to a triplet (J = 6.5 Hz); the integral ratio for the δ 2.3 signal to the signals at δ 1.97 and 1.8 (q, CH_2–CH_2CH_2) decreased from 2/2 to 2/1; IR 2580 (C≡C–D stretch vs. 3300 in C≡C–H, ν_H/ν_D = 1.28), 1980 (C≡CD vs. 2120 for C≡CH, ν_H/ν_D = 1.07), 1015 (overtone of C≡C–D bend vs. 1370 for C≡C–H, ν_D/ν_H = 1.35), 490 cm^{-1} (C≡C–D bend vs. 625 for C≡C–H, ν_C/ν_H = 1.28).

Polymerization of 1,6-Heptadiyne. The reactor vessel of Figure 1 was removed from the drying oven and attached to the vacuum line and evacuated overnight (typically to 10^{-5}–10^{-4} torr). About 12 mL of degassed pentane or toluene was distilled into the 25-mL side bulb. Then 0.3 mL of 1,6-heptadiyne was distilled into the 1-mL graduated side arm. The reactor was closed and transferred into the glovebox. The catalyst was prepared in the glovebox at 25 °C. Typically 0.35 mL of 25% $Al(C_2H_5)_3$ in toluene was added to 60 μL of $Ti(OC_4H_9\text{-}n)_4$. After 60 min at 25 °C the catalyst was degassed at least 6 times by pumping at −78 °C and then allowing the solution to warm to 25 °C under static vacuum. The reactor was then sealed and removed from the vacuum line. The main body of the reactor and the monomer side arm were separately thermostated in appropriate baths. The reactor was removed from the baths only long enough to coat the walls of the reactor with catalyst. Once the reactor was back in the baths, the monomer was admitted to the reactor. The film started to grow within a few seconds and within a few minutes all the monomer had distilled. After 30–60 min the wash solvent in the side bulb was decanted into the reactor. The film was washed and the wash solution was decanted back to the side bulb. Then the solvent was distilled back into the reactor by cooling the reactor with dry ice–acetone. The film was removed from the reactor walls by plunging the reactor into liquid nitrogen. Washing continued until the wash solution was colorless and then for at least six more washes. Typically a total of 20–30 washes was required. After the last wash, the film was dried on the vacuum line. The film was removed from the reactor in the glovebox.

***syn*- and *anti*-1-Ethylidyne-3-methyl-2-cyclohexene (10) and (11).** To a stirred solution of 41.7 mL of 2.4 M *n*-butyllithium (0.100 mol) in hexane and 200 mL of anhydrous ether under argon was added 37.1 g (0.100 mol) of ethyltriphenylphosphonium bromide. The mixture was stirred at 25 °C for 4 h. Then 11.5 g (0.105 mol) of 3-methyl-2-cyclohexen-1-one was added dropwise. The mixture was stirred overnight, refluxed 4 h, cooled, and filtered. The solid was washed with ether and the combined ether filtrates were washed with H_2O until neutral, dried over Na_2SO_4 and concentrated to 8.81 g (72%) of pale yellow liquid with some crystals. Distillation gave bp 61 °C/62 torr or bp 168–170 °C/760 torr, $n^{20°C}_D$ = 1.5051. Elemental analysis. Calcd: C, 88.45; H, 11.55. Found: C, 88.31; H, 11.62. ^1H NMR ($CDCl_3$) δ 1.65 (d, J = 7 Hz, =CHCH_3), 1.73 (s, C–CH_3), 1.7–2.4 (m, $CH_2CH_2CH_2$), 5.21 (q, J = 7 Hz, =C*H*–CH_3), 5.82 (s, 0.83 H, C=CH–C=), 6.20 (s, 0.17 H, C=CH–C=); ^{13}C NMR ($CDCl_3$) δ 12.3, 13.0 (C–CH_3's), 22.8, 23.6 (CH*C*H$_3$'s), 23.8, 24.3, 24.4, 30.8, 31.4, 32.0 (CH_2's), 116.9, 118.7 (C=*C*H–C=), 120.2, 126.7 (C=*C*H–CH_3's), 135.0, 135.2 (=C<), 136.4, 138.0 (=C<); integral ratios 12.3/13.0, 116.9/118.7, 120.2/126.7, and 138.0/136.4 are all about 19/81. The mixture is therefore deduced to be about 80% **10** and 20% **11** by analogy to similar compounds' NMR shifts.[49]

1-Methylene-3-methyl-2-cyclohexene (12). Utilization of the above procedure with 35.7 g (0.100 mol) of methyl triphenylphosphonium bromide led to 9.8 g (93%) of crude product. Rapid distillation (5 min) through a 4-in. jacketed Vigreaux column, followed by rapid distillation (5 min) through a short path still yielded a liquid: bp 26 °C/7.0 torr or 45 °C/12 torr; $n^{20°C}_D$ = 1.4949; reported[50] bp 128–135 °C/730 torr, $n^{20°C}_D$ = 1.4693; ^1H NMR ($CDCl_3$) δ 1.74 (s, CH_3), 1.6–2.4 (m, CH_2's), 4.64 (s, 2 H, =CH_2), 5.92 (s,, 1 H, C=CH–).

1,3-Dimethyl-1,3-cyclohexadiene (13). Slow distillation (1.5 h) of the above reaction product through a short path still yielded a liquid of bp 60 °C/54 torr and $n^{20°C}_D$ = 1.4770 (reported[50] $n^{20°C}_D$ = 1.4776).

Chlorination of Poly(1,6-heptadiyne). A 3 × 3 cm, 9.02-mg (0.0979-mmol) piece of poly(1,6-heptadiyne) was exposed to chlorine gas (~5 mol) on an argon stream over a period of 15 h. Argon was then purged through the flask for several hours and the sample was pumped over a 30-min period to 1 × 10^{-4} torr. The sample, which had changed from lustrous, opaque golden green to nearly colorless, weighted 18.52 mg: IR 2950 (C–H stretch), 1600 (C=C stretch), 1430 (CH_2 scissor), 920 (C=C–H), 780 cm^{-1} (C–Cl). Elemental analysis. Calcd for

(46) J. H. Edwards and W. J. Feast, International Conference on the Physics and Chemistry of Conductive Polymers, Les Arcs, France, Dec 11–15, 1982; *J. Phys.* (*Orsay, Fr.*), in press. D. Bott, British Petroleum Co., personal communication.

(47) G. B. Street, R. H. Geiss, V. Lee, and P. Pfluger, International Conference on the Physics and Chemistry of Conducting Polymers, Les Arcs, France, Dec 11–15, 1982; *J. Phys.* (*Orsay, Fr.*), in press.

(48) K. D. Cummings, D. B. Tanner, and J. S. Miller, *Phys. Rev. B*, **24**, 4142 (1981).

(49) G. Zon and L. A. Pacquette, *J. Am. Chem. Soc.*, **96**, 215 (1974).

(50) A. F. Thomas and M. Stoll, *Chem. Ind.* (*London*), 1491 (1963).

$C_7H_7Cl_3$: C, 42.57; H, 3.57; Cl, 53.86. Found: C, 42.79; H, 3.40; Cl, 52.70; ash, 1.29. Found (corrected for ash): C, 43.27; H, 3.44; Cl, 53.29%.

Doping of Poly(1,6-heptadiyne). (a) Iodine. Samples were attached to four Pt wires with Electrodag conductive adhesive in the glovebox. The Pt wires were fused into a glass cap which fit the doping vessel. The closed assembled doping vessel containing other pieces of film was then removed from the glovebox and attached to an argon line and iodine vapor was admitted on the argon stream. Alternatively, a vacuum-sealed ampule containing degassed iodine and equipped with a break seal was placed in the doping vessel in the glovebox. The doping vessel was evacuated on the vacuum line and isolated. Then, the break seal was broken by means of a magnet to release the iodine. The low-temperature (−78 °C) doping experiment was carried out by using 8 mL of a saturated solution of iodine in toluene prepared at −78 °C to cover a 4 × 11 mm 60 μm thick film; the doping was carried out in a dry ice–acetone bath under argon.

(b) AsF_5. The sample was mounted in a doping vessel as described above. This vessel was attached to the vacuum line and to a flask containing AsF_5 at a pressure of 350 torr. The apparatus was then isolated from the vacuum line and the valve to the AsF_5 opened. At the completion of the experiment the doping vessel was evacuated again to remove excess AsF_5, prior to handling in the glovebox.

Acknowledgment. This research supported in part by the National Science Foundation through Grant DMR-824069.

Registry No. $Al(C_2H_5)_3$, 97-93-8; $Ti(O\text{-}n\text{-}C_4H_9)_4$, 5593-70-4; $Ti(O\text{-}i\text{-}C_3H_7)_4$, 546-68-9; $Ti(O\text{-}n\text{-}C_9H_{19})_4$, 6167-42-6; AsF_5, 7784-36-3; $Al(CH_3)_3$, 75-24-1; $Al(i\text{-}C_4H_9)_3$, 100-99-2; poly(1,6-heptadiyne), 30523-92-3.

Chemical Properties of Phenanthrolinequinones and the Mechanism of Amine Oxidation by *o*-Quinones of Medium Redox Potentials

Timothy S. Eckert and Thomas C. Bruice*

Contribution from the Department of Chemistry, University of California at Santa Barbara, Santa Barbara, California 93106. *Received November 19, 1982*

Abstract: The protonic acid–base properties, equilibria for hydroxide-mediated hydrations and ring contraction, and electrochemistry of the three isomeric phenanthroline-5,6-quinones [1,10 (**1**), 1,7 (**2**), and 4,7 (**3**)] are reported and discussed. Pyridine nitrogens peri to the *o*-quinone carbonyl groups increase the equilibrium constants for addition of H_2O and MeOH to the latter (**3** > **2** > **1**). The reductions of the phenanthroline-5,6-quinones by 1-phenylethanols, hydrazine, cyclohexylamine, glycine, morpholine, and *N,N*-dimethylbenzylamine have been examined. In general the order of the rate of substrate oxidation is **3** > **2** > **1**. Various mechanisms for amine oxidation by high-potential quinones (such as 2,3-dichloro-5,6-dicyano-1,4-benzoquinone) and low- or medium-potential quinones (such as **1**, **2**, and **3**) are discussed, and it is concluded that the mechanisms are different. Hydrazine and *N,N*-dimethylbenzylamine reduce the phenanthrolinequinones to the corresponding quinols. The oxidation of *N,N*-dimethylbenzylamine is catalyzed by the amine-free base and hydroxide ion. The oxidations of cyclohexylamine (to cyclohexanone) and glycine provide 5-amino-6-hydroxyphenanthrolines while the oxidation of morpholine provides the aminoquinol **5**. The nature of the quinone reduction products and the involvement of general base catalysis establish that the quinone plus amine redox reactions proceed via the covalent addition of amine to quinone followed by α-proton removal by general base catalysis.

The mechanisms by which quinones are reduced by organic substrates have been and remain of paramount importance. The possible mechanisms include consecutive one-electron transfers involving a radical pair intermediate two-electron transfer requiring the formation of a covalent intermediate of quinone and substrate, and hydride transfer. These various possibilities were considered and discussed by Hamilton in 1971.[1] High-potential quinones are of use as oxidants in organic synthesis, and attention has been given to the mechanisms of reduction of these reagents (see Discussion). Very little attention has been paid to the mechanisms of organic substrate oxidations by quinones of moderate redox potentials. Corey and Achiwa[2] realized that such quinones could be useful reagents in the oxidation of amines to ketones and studied the oxidation of cyclohexylamine by 3,5-*tert*-butylbenzo-1,2-quinone. This *o*-quinone was employed to obviate competing 1,4-additions of amine to the quinone oxidant. Jackman in 1960[3] proposed that phenanthrene-4,5-quinone should be investigated as an oxidant since it could not undergo 1,4-addition of nucleophilic substrates. To our knowledge this suggestion has never been followed.

In this study we have investigated the phenanthrolinequinones **1**, **2**, and **3**. They possess the advantage that Jackman appreciated

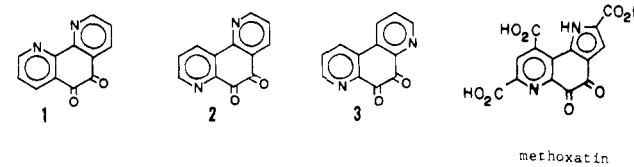

in the phenanthrene-*o*-quinone but possess more positive potentials than the latter (vide infra). In addition, quinones **1**, **2**, and **3** bear an obvious structural similarity to the natural product methoxatin, a bacterial coenzyme for the enzymatic oxidation of alcohols, glucose, aldehydes, and methylamine.[4] Among other findings, there is presented evidence that the oxidation of amines occurs via formation of carbinolamine and imine intermediates and that

(1) Hamilton, G. A. "Progress in Bioorganic Chemistry"; Kaiser, E. T., Kezdy, F. J., Eds.; Wiley: New York, 1971; Vol. 1, pp 83–157.
(2) Corey, E. J.; Achiwa, K. *J. Am. Chem. Soc.* **1969**, *91*, 1429–1432.
(3) Jackman, L. M. *Adv. Org. Chem.* **1960**, *2*, 329–365.
(4) Salisbury, S. A.; Forrest, H. S.; Cruse, W. B. T.; Kennard, O. *Nature (London)* **1979**, *280*, 843–844. Forrest, H. S.; Salisbury, S. A.; Sperl, G. *Biochim. Biophys. Acta* **1981**, *676*, 226. Duine, J. A.; Frank, J.; Van Zeeland, J. K. *FEBS Lett.* **1979**, *108*, 443–446. Ameyama, M.; Matsushita, K.; Ohno, Y.; Shinagawa, E.; Adachi, O. *Ibid.* **1981**, *130*, 179–183. De Beer, R.; Duine, J. A.; Frank, J.; Large, P. J. *Biochim. Biophys. Acta* **1980**, *622*, 370–374. Mincey, T.; Bell, J. A.; Mildvan, A. S.; Abeles, R. H. *Biochemistry* **1981**, *20*, 7502–7509.

0002-7863/83/1505-4431$01.50/0